Volume 2 | Number 47 | 21 December 2014 | Pages 8259–8442

Journal of Materials Chemistry B

Materials for biology and medicine

www.rsc.org/MaterialsB

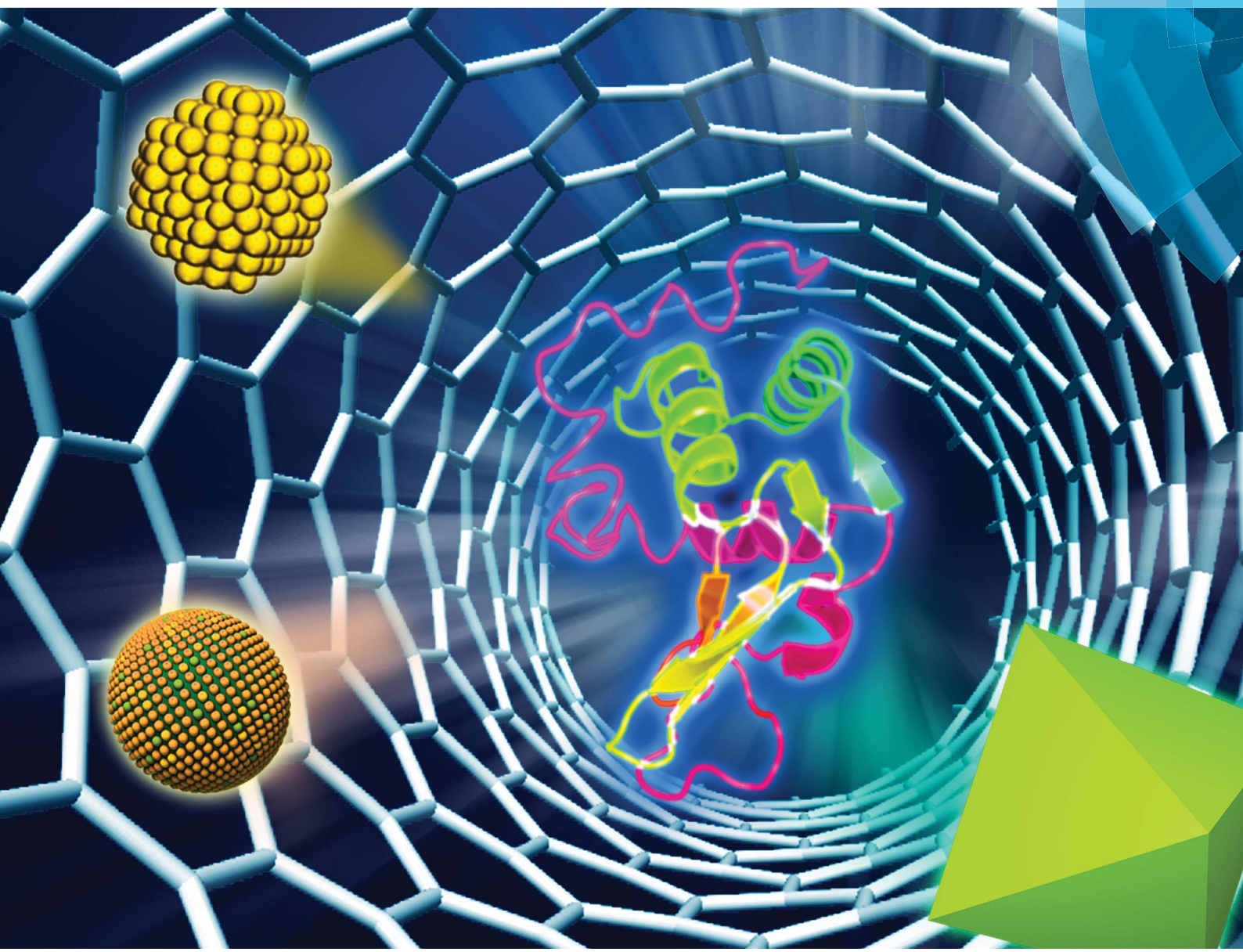

ISSN 2050-750X

ROYAL SOCIETY OF CHEMISTRY

FEATURE ARTICLE

Hui Wei *et al.*

Protein-directed approaches to functional nanomaterials: a case study of lysozyme

Journal of Materials Chemistry B

FEATURE ARTICLE

View Article Online
View Journal | View Issue

Cite this: J. Mater. Chem. B, 2014, 2, 8268

Protein-directed approaches to functional nanomaterials: a case study of lysozyme†

Yubin Ding, Leilei Shi and Hui Wei*

Received 26th July 2014
Accepted 25th September 2014

DOI: 10.1039/c4tb01235f

www.rsc.org/MaterialsB

Functional nanomaterials have found wide applications in diverse areas because of their intrinsically different properties compared to their bulk counterparts. To achieve the goal of preparing functional nanomaterials, various strategies have been successfully developed. Among them, the biomolecule-directed approach has been extensively explored to synthesize many functional nanomaterials owing to their programmability, self-assembly and recognition capabilities. This Feature Article highlights the use of lysozyme as a model protein to the direct synthesis of nanomaterials. Future advances in rational *de novo* design and synthesis of functional nanomaterials with proteins will depend on a deep understanding of the synthetic strategies and the formation mechanisms. This Feature Article discusses the synthesis of nanomaterials with lysozyme in both the solution phase and crystal form. The synthetic strategies, formation mechanisms and wide applications of several kinds of materials, such as metals, oxides, metal sulfides, and composites, are covered. The lessons from this case study will provide invaluable guidance in future materials design using proteins and other biomolecules. Rational design of personalized functional nanomaterials will be possible in the future (366 references).

1. Introduction

Functional nanomaterials have found wide applications in various areas, from catalysis, energy conversion and storage, information science, to environmental and biomedical science because of their intrinsically unique properties compared to their bulk counterparts.[1–93] To achieve the goal of synthesizing functional nanomaterials, numerous innovative approaches have been developed. Among them, biomolecule-directed approaches have been extensively explored to prepare a variety of functional nanomaterials owing to their programmability, self-assembly and recognition capabilities.[94–153] In particular, proteins provide several distinct characteristics for nanomaterial fabrication, including their nanoscaled sizes, distinctive molecular structures, diverse functionality, highly-specific biorecognition, and various self-assembly abilities. In addition, proteins with the designed structures and functions can be obtained through protein engineering. Moreover, atomic resolution structural information can be provided *via* protein

Department of Biomedical Engineering, Aerosol Bioeffects and Health Research Center, College of Engineering and Applied Sciences, Nanjing National Laboratory of Microstructures, Nanjing University, Nanjing, Jiangsu, 210093, China. E-mail: weihui@nju.edu.cn; Fax: +86-25-83594648; Tel: +86-25-83593272

† Electronic supplementary information (ESI) available. See DOI: 10.1039/c4tb01235f

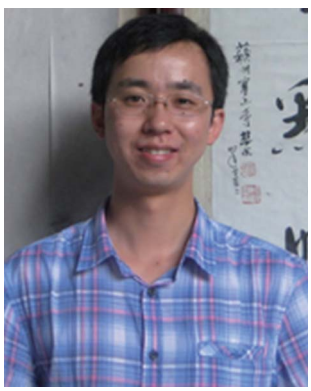

Yubin Ding received his B.S. degree in applied chemistry from Shanxi University in 2008 and Ph.D. degree in applied chemistry from East China University of Science & Technology in 2013. Currently, he is a research assistant professor in Professor Hui Wei's group at Nanjing University. His research interests are focused on the design and synthesis of fluorescent probes for biomedical applications.

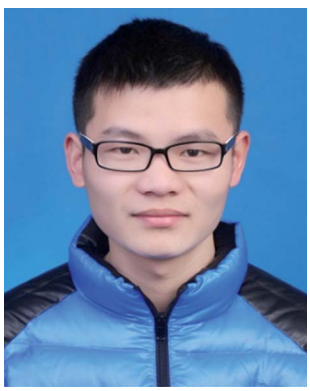

Leilei Shi received his B.S. degree in materials physics from Nanjing University in 2014, where he carried out undergraduate research with Professor Hui Wei. Currently, he is a graduate student in Professor Hui Wei's group at Nanjing University. His research interests are focused on the design and synthesis of functional nanomaterials for biomedical applications.

crystallography, allowing for mechanism studies. Proteins, in the form of monomers, assemblies, and even single crystals, can direct the formation of many functional materials, such as metal nanoclusters, metal nanoparticles, metal oxides, silica, semiconductor quantum dots, conducting polymers and reduced graphene oxide.[108–121,154–166] Despite the significant advances, the rational design and preparation of functional nanomaterials with intentionally desired properties remain a great challenge in the field due to the incomplete understanding of the nanomaterial formation mechanism and protein–nanomaterials interactions.[159]

To address these challenges and highlight the significant progress in the field, this feature article discusses the uses of lysozyme as a model protein to prepare various nanomaterials, to elucidate the growth mechanism and protein–nanomaterials interactions, and to demonstrate the key applications (note: lysozyme used throughout this paper is from chicken egg white unless otherwise specified) (Fig. 1). Unlike other model proteins, such as bovine serum albumin, ferritin and caged virus proteins, lysozyme is a relatively small protein with 129 amino acid residues and a calculated molecular weight of 14 307 Da,[167] which allows easier access for characterization and manipulation. Lysozyme has 8 cysteine residues, forming 4 disulfide bonds, and 1 surface-exposed histidine residue (Fig. S1†). Lysozyme is also relatively easy to crystallize, allowing for atomic resolution examinations of the structure.[159,162,168] In addition, lysozyme is an enzyme that enables studies of its biological activity after forming nanomaterials and the preparation of multifunctional materials (Fig. S2†). In addition, lysozyme is stable over wide temperature and pH ranges, making it suitable for a variety of synthetic approaches. This article summarizes both lysozyme in the solution phase-directed approach and lysozyme crystal-directed approach to functional nanomaterials. First, the synthesis and careful characterization of metal nanoclusters (such as gold, silver, copper, platinum, and bimetallic nanoclusters) in the solution phase are discussed. The possible growth mechanisms are also explored with the aid of detailed kinetic and mass spectroscopic studies. In addition to applications in sensing and tumour cell detection, a biological activity study of lysozyme after forming nanoclusters is also covered. Studies of large metal nanoparticles and other materials in solution phase are then summarized. Their formation mechanism, antimicrobial activity, assembly and numerous applications are investigated. In Section 3, the use of lysozyme crystals (both cross-linked crystals and intact single crystals) to direct the synthesis of different kinds of hybrid nanomaterials, from plasmonic metal nanomaterials and fluorescent quantum dots to magnetic nanoparticles and conducting polymers, is discussed. The growth mechanisms and structure evolution are elucidated using a combination of electron microscopy with tomography, X-ray crystallography, and other techniques. The development of effective methods to tune the nanomaterial properties, such as the optical and magnetic properties, is presented. Several interesting applications, including plasmonic and catalytic applications, are also described. Finally, the current challenges, opportunities and perspectives in rational materials design using lysozyme and other proteins are discussed.

The readers are referred to numerous excellent reviews for more comprehensive information regarding the synthesis of functional nanomaterials with other proteins and biomolecules rather than lysozyme (note: due to the limited space, only a small number of reviews are cited in the references).[173–191] Under certain conditions, lysozyme itself can also form innovative functional materials and be engineered for diverse exciting applications.[192–196] Using target proteins (such as lysozyme) as a template, molecularly imprinted polymers have been successfully *in situ* coated onto supporting nanoparticles (*e.g.*, magnetic or silica nanoparticles) to construct core–shell structured functional materials for the selective recognition and enrichment of target proteins.[197–204] These topics, however, are beyond the scope of the current review and will not be covered.

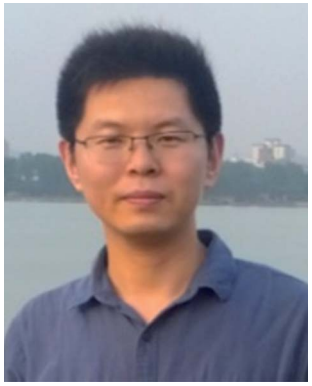

Hui Wei received his B.S. degree in chemistry from Nanjing University in 2003 (advisor: Professor Xinghua Xia) and Ph.D. degree in chemistry from Changchun Institute of Applied Chemistry, Chinese Academy of Sciences in 2008 (advisor: Professor Erkang Wang). After postdoctoral training with Professors Yi Lu and Shuming Nie, he joined Nanjing University and started his independent career. Currently, he is a Professor at Nanjing University. His research interests are focused on the design and synthesis of functional nanomaterials and the development of new methodologies for analytical and biomedical applications.

2. Lysozyme in solution phase

In this section, the use of lysozyme to direct formation of functional nanomaterials in solution phase is discussed.

2.1 Metal nanoclusters

Metal nanoclusters, consisting of a few to several hundred metal atoms with sizes smaller than 2 nm, have received considerable attention because of their ultrasmall and atomically precise size, nontoxicity, and unique physical, electrical, electrochemical, catalytic, and optical properties.[156,184,205–289] They have already found wide applications in many areas, such as bioconjugation, catalysis, nanodevices, bioimaging, biosensing, and cancer therapy. Researchers have established that proteins, including lysozyme, can direct the formation of metal nanoclusters.[113,116,117,120,146,154,155,234,290–304] Compared to other methods developed to date, the protein-directed approach can produce metal nanoclusters with good water solubility, high stability, strong fluorescence, biocompatibility and biofunctionality. The method is also environmentally friendly and the nanoclusters formed are ready for further bioconjugation.

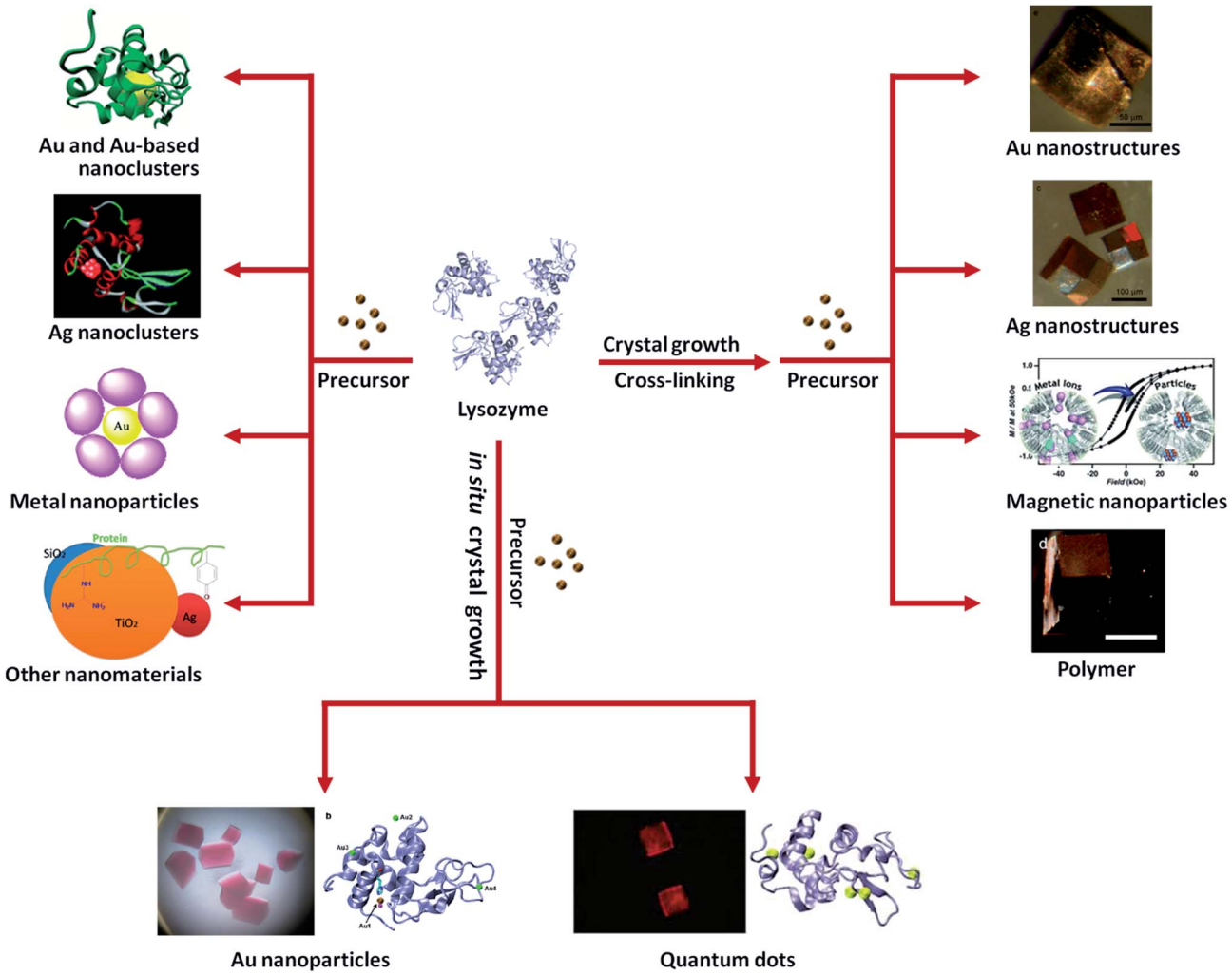

Fig. 1 Lysozyme-directed approaches to functional nanomaterials. (left) Solution phase-directed approach, (right) cross-linked crystal-directed approach, and (bottom) intact single crystal-directed approach to functional nanomaterials. From the upper right to upper left (clockwise): reprinted with permission from ref. 114, copyright (2010) John Wiley and Sons; ref. 169, copyright (2012) John Wiley and Sons; ref. 164, copyright (2012) Royal Society of Chemistry; ref. 162, copyright (2013) Tsinghua University Press and Springer; ref. 159, copyright (2011) Nature Publishing Group; ref. 170, copyright (2013) American Chemical Society; ref. 171, copyright (2007) American Chemical Society; ref. 172, copyright (2012) Royal Society of Chemistry; ref. 155, copyright (2010) Royal Society of Chemistry.

Several kinds of metal nanoclusters, including Au, Ag, Cu, Pt, and bimetallic nanoclusters, have been synthesized *via* lysozyme-directed approaches.[121,155,172,299,305–313]

2.1.1 Au

Synthetic protocols. Previous work has shown that fluorescent Au nanoclusters can be formed under basic conditions using bovine serum albumin (BSA) as both the reducing agent and capping ligand.[154] It is suggested that metal ions can be reduced by tyrosine (and/or tryptophan) residues through the phenolic groups. Inspired by this interesting discovery, Wei and co-workers demonstrated for the first time that highly fluorescent Au nanoclusters could be synthesized in basic aqueous solutions using lysozyme as the reducing and stabilizing agent (Fig. 2A).[155] The Au nanoclusters were formed after incubation of a mixture of $HAuCl_4$ and lysozyme at 37 °C under basic conditions due to the reduction of $HAuCl_4$ by tyrosine (and/or tryptophan) residues of lysozyme. The optimal synthetic

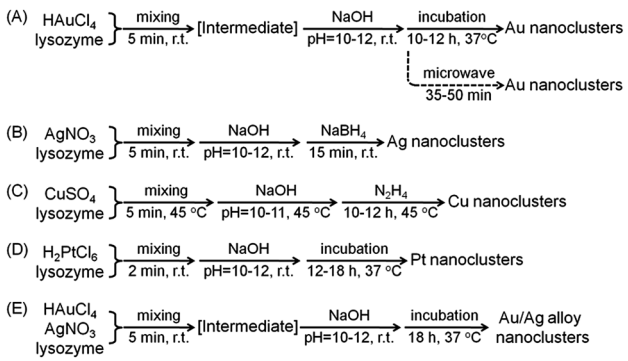

Fig. 2 Synthetic protocols for metal nanoclusters with lysozyme in aqueous solutions. (A) Au nanoclusters,[155,305] (B) Ag nanoclusters,[172] (C) Cu nanoclusters,[299] (D) Pt nanoclusters,[313] and (E) Au/Ag bimetallic alloy nanoclusters.[315] r.t. = room temperature.

approach could be obtained by optimizing the molar ratios of lysozyme to $HAuCl_4$, the concentrations of lysozyme, $HAuCl_4$ and NaOH, the reaction time and incubation temperature. Molar ratios of 0.17 : 1 and 0.18 : 1 of lysozyme to $HAuCl_4$ were used by Wei *et al.* and Xu *et al.*, respectively.[155,310] Higher molar ratios were also employed by others.[306,309] Most reports adopted Wei *et al.*'s approach to prepare lysozyme stabilized Au nanoclusters.[121,306–309,312] Chen's group showed that the reaction time could be significantly shortened from several hours to less than 1 hour by microwave heating instead of 37 °C incubation (Fig. 2A).[305,314] It should be noted that microwave irradiation was applied intermittently to prevent overheating. Lin and Tseng showed that lysozyme from different vendors produced Au nanoclusters with different quantum yields, suggesting that salt and other small molecular contaminants may affect the synthesis.[306]

Characterization and mechanism. The formation of Au nanoclusters can be indicated and easily monitored by the appearance of a yellow-brown colour. Unlike monolayer protected Au nanoclusters, the lysozyme stabilized Au nanoclusters usually do not exhibit well-defined spectroscopic features (*i.e.*, step-like fine structures) in the UV-visible absorption spectra, even though an absorption band centred at 400 nm was observed.[306] The band of 400 nm was assigned to Au $5d^{10}$ to 6sp inter-band transitions and/or ligand–metal charge-transfer transitions.[306]

The formation of Au nanoclusters can be further confirmed and their sizes can be characterized by transmission electron microscopy (TEM), dynamic light scattering (DLS) and mass spectroscopy (MS).[155,306,309,310,312] Owing to the ultrasmall sizes of the Au nanoclusters, high resolution TEM was usually employed.[155,309,310,312] The size of the Au nanoclusters was around 1 nm under TEM (Fig. 3).[155] Nanoparticles as large as 4 nm were also observed, which probably originated from the by-products (*i.e.*, Au nanoparticles) rather than the Au nanoclusters.[312] The larger sizes measured by TEM might be also due to the electron beam-induced *in situ* aggregation of Au nanoclusters (or TEM sample preparation-induced aggregation).

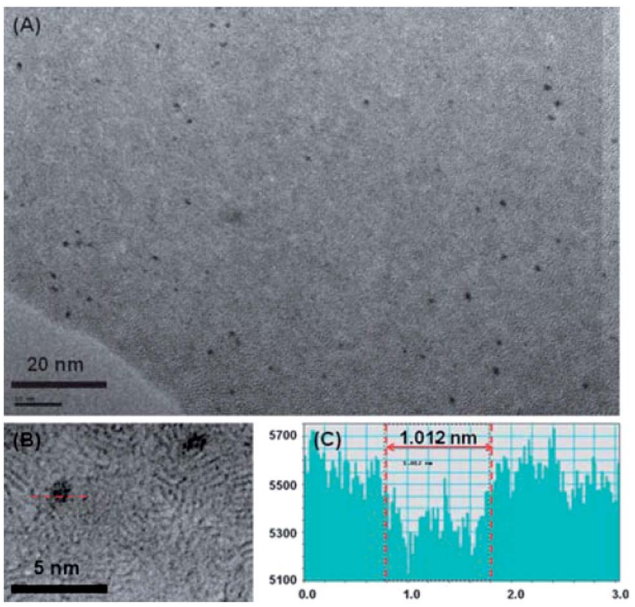

Fig. 3 Typical TEM image of lysozyme stabilized Au nanoclusters (A) and (B) higher magnification image of panel (A) and (C) corresponding size of the particle line-crossed in panel (B). Reprinted with permission from ref. 155, copyright (2010) Royal Society of Chemistry.

The hydrodynamic sizes were measured by DLS.[306] Hydrodynamic sizes of 5, 7, 8, and 28 nm were reported, which was strongly dependent on the molar ratio of lysozyme to $HAuCl_4$.[306] Only Au nanoclusters with a hydrodynamic size of 8 nm were discussed, which were prepared with a 0.17 : 1 molar ratio of lysozyme to $HAuCl_4$. Based on the dimensions of lysozyme from the crystal structure (*i.e.*, 4.5 nm × 3.0 nm × 3.0 nm), it was suggested that a lysozyme monolayer was formed on the Au nanocluster core.[306] This explanation, however, was inconsistent with the experimental results, which showed that the hydrodynamic sizes decreased from 28, 8, 7 to 5 nm when the molar ratios of lysozyme to $HAuCl_4$ were increased from 0.14 : 1, 0.17 : 1, 0.21 : 1 to 0.28 : 1.[306] The explanation was also inconsistent with recent studies, which suggested that the Au nanocluster core was encapsulated within a lysozyme.[309,310] If a monolayer of lysozyme proteins was formed onto the Au nanocluster core, the hydrodynamic size would increase with increasing lysozyme to $HAuCl_4$ molar ratio. Here, we propose that each Au nanocluster was probably encapsulated within a lysozyme based on the previous studies.[306,309,310] This is in agreement with the measured hydrodynamic size of 5 nm for the Au nanoclusters from the 0.28 : 1 molar ratio of lysozyme to $HAuCl_4$. For Au nanoclusters with large hydrodynamic sizes, the increased sizes might have originated from the aggregation of the Au nanoclusters encapsulated lysozyme due to salt or metal ions bridging.[309]

MS is one of the most suitable and powerful tools to elucidate the "actual molecular formulae" of ultrasmall nanoclusters.[219] Previous studies have demonstrated that various ionization modes can be used for nanoclusters MS analysis, such as electrospray ionization (ESI), laser desorption ionization (LDI), and matrix-assisted laser desorption ionization (MALDI).[219] Among them, ESI-MS is the mildest mode with lowest fragmentation. Despite this, the presence of metal nanoclusters makes the ESI-MS analysis of proteins quite challenging. Therefore, MALDI mode, combined with time-of-flight (TOF), is frequently employed in analyzing protein stabilized nanoclusters, including lysozyme stabilized metal nanoclusters.[121,306,309,311,316] Based on the MALDI data, Tseng and co-workers assigned a Au_{25} formula to the Au nanocluster stabilized by lysozyme, which emitted red fluorescence centered at ~657 nm (Fig. 4).[121,306] As shown in the time-dependent fluorescent evolution profile in Fig. 4, another emission peak centered at ~445 nm was observed, which was assigned to Au_8 by Tseng *et al.*[121] Because multiple MALDI peaks with a spacing of m/z 197 were detected for both the fluorescent species at 445 nm and 657 nm (referred as "blue fluorescent species" and "red fluorescent species", respectively), the two species were assigned to Au_8 and Au_{25} based on the Jellium model, respectively.[121] According to the model, the most stable metal clusters should have a magic number of atoms.[121] Later, Pradeep *et al.*

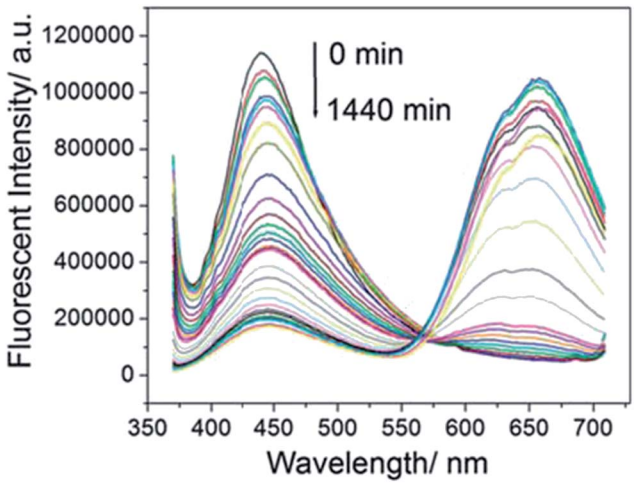

Fig. 4 Time-dependent fluorescent spectra of lysozyme-stabilized Au fluorescent cluster. The excitation wavelength was 360 nm. Reprinted with permission from ref. 155, copyright (2010) Royal Society of Chemistry.

performed a more detailed MALDI-MS analysis of the lysozyme stabilized Au nanoclusters.[309] For the "red fluorescent species", an m/z shift of 1970 from lysozyme alone was observed, suggesting the presence of 10 Au atoms within a single lysozyme (Fig. 5). Therefore, it was claimed that a cluster of the Au_{10} core was formed within a lysozyme protein. Careful analysis of the MALDI MS spectra in the entire mass range suggested that each Au nanocluster was confined within a lysozyme protein rather than grown between a few proteins.[309] For "blue fluorescent species" made by incubating lysozyme and $HAuCl_4$ before exposure to basic conditions, Pradeep and co-workers detected a maximum of 3 Au atoms bound to a lysozyme using ESI MS.[309] The discrepancy of the MS results between the above studies should be due to the typical fragmentation by MALDI, which complicates the assignments.[219] Thus, more convincing data

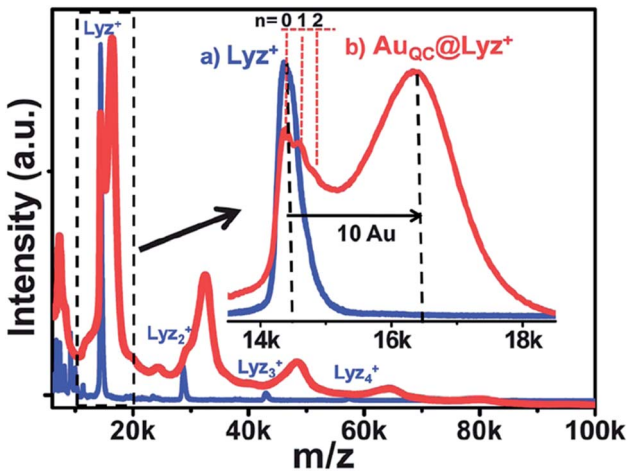

Fig. 5 MALDI MS spectra of lysozyme (blue curves) and lysozyme-stabilized Au fluorescent nanocluster (red curves). Reprinted with permission from ref. 309, copyright (2013) Royal Society of Chemistry.

from other methods, such as crystallography, is needed to clarify the exact formulae of metal nanoclusters.

Nevertheless, as proposed by Wei *et al.* and echoed by Tseng's and Pradeep's groups, the following growth mechanism can be proposed: the mixing of lysozyme and $HAuCl_4$ at acid pH forms intermediate species with blue fluorescence; it then converts to the final red fluorescence species when incubated at basic pH (Fig. 2A and 6).[121,155,306,309] More specifically, when lysozyme and $HAuCl_4$ are mixed at low pH, Au^{3+} binds to lysozyme by coordinating with the O and N atoms of the amino acids. The lysozyme–$(Au^{3+})_m$ complexes are then reduced to lysozyme–$(Au^{+})_m$ probably by the carboxyl groups of acidic amino acids, as revealed by X-ray photoelectron spectroscopy (XPS) (*vide infra*), which would emit blue fluorescence. For lysozyme–$(Au^{+})_m$, Au^{+} may assemble together due to aurophilic attraction. At high pH, Au^{+} in lysozyme–$(Au^{+})_m$ is reduced to Au^0, which would further assemble into lysozyme–$(Au^0)_{m+n}$.[121,155,306,309] Inter-protein metal ion transfer was suggested because the regeneration of free lysozyme was detected during time-dependent MS analysis.[309] Circular dichroism (CD) indicated that lysozyme at high pH had a more partially unfolded structure (*i.e.*, less α-helical structure content) than lysozyme at low pH. The further unfolding of lysozyme would provide larger internal space for encapsulating an enlarged Au nanocluster (Fig. 6).[121] It was suggested that amine groups and the thiol groups of cysteine were involved in stabilizing the formed Au nanocluster within lysozyme.[309,310]

The photoluminescence quantum yields of the "red fluorescent species" were reported by several groups, ranging from 5.2% to 15.6%.[155,306,309,310,312] The variations might be due to the different measurement conditions as well as the quality of the nanoclusters synthesized. Lifetime measurements were also

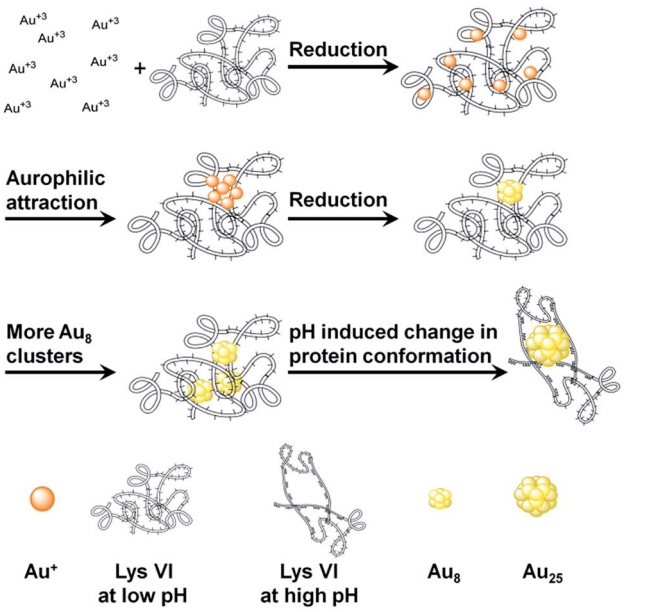

Fig. 6 Proposed growth mechanism of lysozyme-stabilized Au fluorescent nanocluster. Adapted with permission from ref. 121, copyright (2012) John Wiley and Sons.

carried out in previous studies, showing the characteristic two lifetime components.[306,309,310]

As discussed above, the XPS data showed that the "blue fluorescent species" should be lysozyme–$(Au^+)_m$. For the "red fluorescent species", the collected XPS spectra could be deconvoluted into two distinct components, *i.e.*, Au^+ and Au^0.[155,306] This indicated that the Au nanoclusters had a Au^0 core and Au^+ shell. For Au_{25} with a Au_{13} core and $12Au^+$, the theoretical value of Au^+ should be 48%. However, most of the measured values were lower, probably due to the X-ray induced *in situ* reduction of Au^+ during the XPS measurements.

In addition to CD spectroscopy (*vide supra*), infrared spectroscopy was also employed to investigate the potential structural changes of lysozyme after forming Au nanoclusters.[305,309,310,312] Although the over spectrum of the lysozyme stabilized Au nanocluster was similar to that of lysozyme alone, a few changes were observed, indicating the increased disordered structures as well as fewer helical components.[305,309,310,312]

It should be noted that the as-prepared Au nanoclusters were stable in NaCl solutions with concentrations as high as 500 mM NaCl and at high pH.[306]

Applications. Owing to the unique fluorescent properties, the Au nanoclusters have been used to develop several sensing systems. As revealed by XPS, Au^+ was present on the outside of the Au nanocluster. Because of the specific Au^+–Hg^{2+} interactions, the red fluorescence of the Au clusters was specifically quenched by Hg^{2+}. Based on this interesting phenomenon, selective and sensitive methods towards Hg^{2+} detection were successfully developed.[155,306] The results showed that CH_3Hg^+ could also be determined with the Au nanoclusters.[306] It should be noted that the red fluorescence of the Au nanoclusters remained unchanged after exposure to glutathione (GSH), further suggesting the formation of a highly stable cluster (*i.e.*, Au_{25}).[121]

Cyanide ions could etch the Au nanoclusters and quench the fluorescence. Based on this, Lu *et al.* employed the nanoclusters as new fluorescent probes to determine cyanide ions.[312]

Zhang's group found that the fluorescence of protein stabilized Au nanoclusters could be enhanced significantly on plasmonic substrates (such as nanostructured silver substrates).[307] The proteins used to direct the formation of Au nanoclusters were BSA, human serum albumin (HSA), egg white albumin (EA), lysozyme, and horseradish peroxidase (HRP). More interestingly, when these five nanoclusters immobilized onto a silver substrate were exposed to different target proteins, they produced distinct fluorescent patterns (Fig. 7). Using this sensing array strategy, as many as 10 proteins at concentrations of 0.2 μM were successfully identified.[307]

As the bioactivity of lysozyme was retained after forming the Au nanoclusters, the lysozyme stabilized Au nanoclusters could recognize and label bacteria, as demonstrated by Chen *et al.*[305] As shown in Fig. 8, the Au nanoclusters could bind to and thus label pan-drug-resistant *Acinetobacter baumannii* (PDRAB) and vancomycin-resistant *Enterococcus faecalis* (VRE), two typical antibiotic-resistant bacteria. The Au nanoclusters also interacted with Gram-negative bacteria and Gram-positive bacteria, such as *E. coli* and *S. aureus*, showing their potential use as

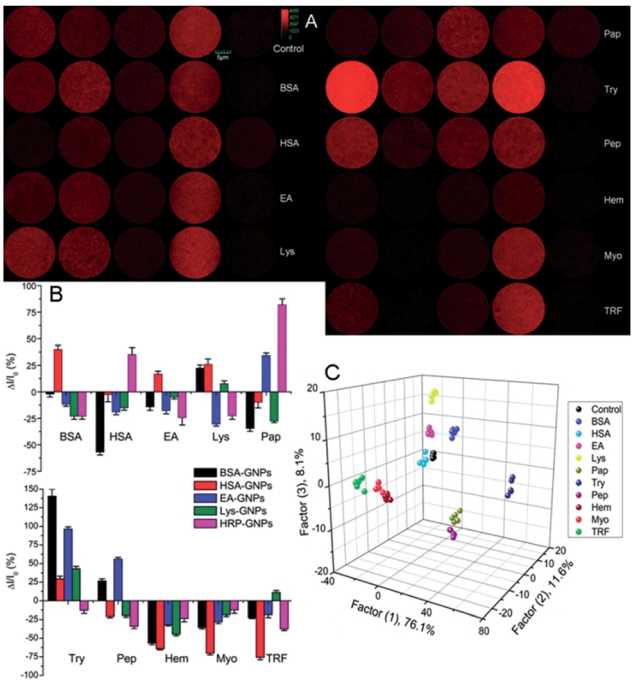

Fig. 7 Combined with others protein stabilized clusters, lysozyme stabilized Au nanoclusters were fabricated into a sensing array on a plasmonic substrate for protein detection. Reprinted with permission from ref. 307, copyright (2012) American Chemical Society.

broad-spectrum labeling probes for pathogenic bacteria.[305] Although the thiols of cysteines and amine groups may be involved in stabilizing the Au nanoclusters, no cysteine is located within the active sites of lysozyme at Glu-35 and Asp-52.[305] Therefore, the lysozyme's bioactivity of the Au nanoclusters was retained, as demonstrated above. When the antimicrobial activity against VRE and PDRAB was examined, it was found that the Au nanoclusters showed better performance (*i.e.*, more effective inhibition of bacteria cell growth) than the free lysozyme.[305] This may have originated from the synergic effects.

Chen *et al.* later showed that lysozyme-stabilized Au nanoclusters could be also used to concentrate the target bacteria. The concentrated bacteria were then analysed and identified by MALDI MS assisted with principal component analysis (PCA). As low as $\sim 10^6$ cells per mL was successfully detected by the proposed method.[314]

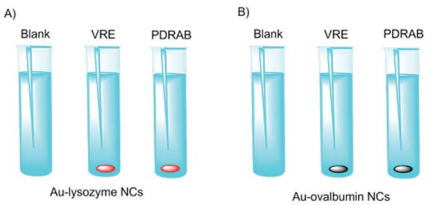

Fig. 8 Lysozyme-stabilized Au nanoclusters for bacterial labeling. The images were taken under illumination of a ~365 nm UV lamp. NC: nanocluster; PDRAB: pan-drug-resistant *Acinetobacter baumannii*; VRE: vancomycin-resistant *Enterococcus faecalis*. Adapted from ref. 305.

Nanozymes are nanomaterials with enzyme-like activity.[33] Recently, it was shown that lysozyme-stabilized Au nanoclusters possessed peroxidase-like activity. When the Au nanoclusters were conjugated onto folic acids functionalized graphene, the conjugates could be used for cancer cell detection. With this sensing platform, as few as 1000 MCF cells were detected.[308]

2.1.2 Ag

Synthetic protocols. Compared to Au nanoclusters, the synthesis of silver nanoclusters is more challenging owing to their intrinsic chemical instability.[117] As promising fluorescent probes, considerable efforts have been devoted to silver nanoclusters preparation recently.[117,210] Several protein-stabilized silver nanoclusters have been synthesized.[115,117,317] As shown in Fig. 2B, a facile approach to red-emitting silver nanoclusters was developed.[172] The synthesis was carried out by reducing silver nitrate with $NaBH_4$ in the presence of lysozyme under basic conditions, which would partially unfold the lysozyme protein and provide more space for encapsulating the nanocluster formed. The alkaline reaction solution would also help to cleave the disulfide bonds and liberate the free cysteines. The freed cysteines could act as a polyvalent ligand to stabilize the silver nanoclusters. As noted, the freshly prepared silver nanoclusters were not stable at high pH. Therefore, they were transferred to a neutral pH solution for long-term storage.[172]

Characterization and applications. The synthesized silver nanoclusters had a size of 1.5 nm under TEM and a hydrodynamic size of 7 nm. No MS spectra have been obtained for the nanoclusters. Owing to the high pI of lysozyme (pI = 11.3), the nanoclusters had a zeta potential of about +30 mV at neutral pH. Interestingly, the silver nanoclusters emitted red fluorescence at 605 nm. A quantum yield of 1.3% was reported.[172] XPS revealed the co-existence of Ag^0 and Ag^+. Because of the specific Ag^+–Hg^{2+} metallophilic interaction, the silver nanoclusters were used as sensitive and selective probes for Hg^{2+} sensing.[172]

2.1.3 Others. Several other metal nanoclusters stabilized by lysozyme were also reported, including copper, platinum and alloy.[299,313,315]

Copper nanoclusters. Blue-emitting copper nanoclusters were synthesized by reducing copper sulphate with hydrazine in the presence of lysozyme under basic conditions (Fig. 2C).[299] TEM indicated that the ~0.96 nm small nanoclusters were aggregated into ~2.3 nm assemblies. The CD and IR spectra again showed disturbed lysozyme structures after forming the copper nanoclusters.[299,305,309,310,312] The fluorescent quantum yield of the emission at 450 nm was measured to be 18% when the nanoclusters were excited at 360 nm. Interestingly, the nanoclusters' fluorescent emission wavelength was dependent on the excitation wavelength (Fig. 9A), indicating that multiple species were present.[299] MALDI MS analysis indeed showed the presence of multiple species, such as Cu_2, Cu_4 and Cu_9 (Fig. 9B).[299] The copper nanoclusters did not show significant cytotoxicity. When co-incubated with cancer cells, such as HeLa cells, the copper nanoclusters were taken up by the cells and could be used for cell labelling and imaging.[299] The preliminary data showed that the copper nanoclusters were stable in blood and did not cause obvious hemolysis.[299]

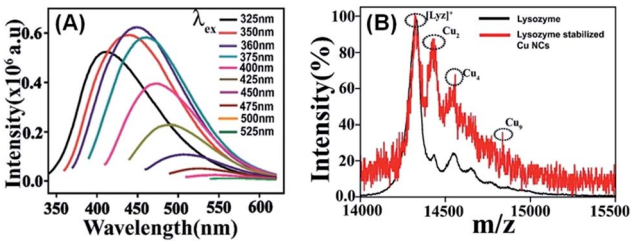

Fig. 9 (A) Fluorescent spectra and (B) MALDI-TOF MS of the lysozyme stabilized copper nanoclusters. Reprinted with permission from ref. 299, copyright (2014) American Chemical Society.

Platinum nanoclusters. The above synthetic protocol was recently extended to platinum nanoclusters.[313] As shown in Fig. 2D, the lysozyme stabilized ultrasmall platinum nanoclusters with blue fluorescence could be formed by incubating lysozyme and H_2PtCl_6 under basic conditions. The platinum nanoclusters were too small to be imaged by TEM. When MALDI TOF MS analysis was conducted, a Pt_4 formula was revealed, confirming the ultrasmall size of the nanoclusters. When excited at 370 nm, the nanoclusters emitted blue fluorescence at 434 nm with a quantum yield of 0.08 and a fluorescence lifetime of 3.0 ns. The fluorescence was excitation wavelength dependent. Similar to the Au nanoclusters mentioned above, the platinum nanoclusters were also composed of 67% Pt^+ and 33% Pt^0, as identified by the XPS measurements. The presence of Pt^0 was further testified by the fact that the platinum nanoclusters' fluorescence could be quenched by Hg^{2+}.[313]

Interestingly, the platinum nanoclusters exhibited intrinsic oxidase-like activity. The platinum nanoclusters could catalyse the oxidation of 2,2′-azino-bis(3-ethylbenzothiazoline-6-sulphonic acid) (ATBS), 3,3′,5,5′-tetramethylbenzidine (TMB), and dopamine in the presence of O_2. The platinum nanoclusters had higher oxidase mimic activity compared to platinum particles larger than 5 nm.[313] The degradation of methylene blue in lake water by the platinum nanoclusters as an oxidase mimic was explored. Methylene blue was indeed degraded in the presence of the platinum nanoclusters, showing great promise in future water treatment.[313]

Alloy nanoclusters. As discussed above, Tseng *et al.* suggested the formation of intermediate Au_8 nanoclusters in the conversion of lysozyme–$(Au^+)_m$ to lysozyme–$(Au^0)_{m+n}$ (*i.e.*, Au_{25}, as proposed by them) (Fig. 2A).[121] Later, they found that the presence of Ag^+ ions in the reaction solution slowed down the conversion, and produced both small and large sized metal nanoclusters simultaneously (Fig. 2E).[315] The formation of alloyed nanoclusters was indicated by the blue shift of the first exciton absorption and fluorescence peaks and confirmed by the MALDI MS analysis. By analyzing the MS spectra, the small nanoclusters were assigned as Au_7Ag and Au_8 while the large ones were assigned as $Au_{24}Ag$. Because the small nanoclusters were insensitive to Hg^{2+} while the large ones were sensitive to Hg^{2+}, a ratiometric fluorescence assay towards Hg^{2+} was proposed (Fig. 10). Such a ratiometric sensing protocol would overcome the potential interfering factors, such as

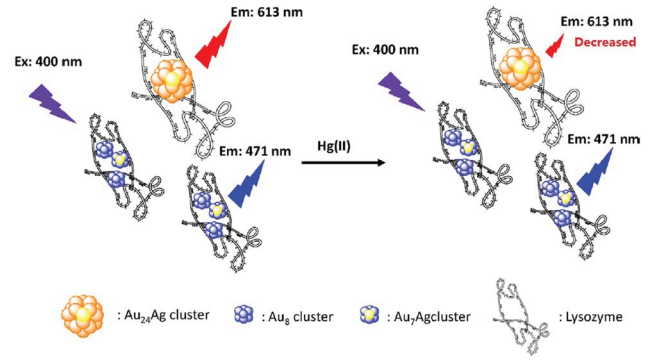

Fig. 10 Ratiometric sensing of Hg^{2+} using two-sized nanoclusters. Reprinted with permission from ref. 315, copyright (2013) Elsevier.

environmental variations and photo bleaching, *etc.* The Hg^{2+} concentration in tap water was evaluated using the proposed assay.[315]

2.2 Metal nanoparticles

Protein-directed approach has also been extensively explored to synthesize varieties of functional metal nanomaterials.[175,182] Nanostructured gold, silver, copper, nickel, cobalt, platinum, and palladium, have been prepared with different proteins such as BSA, bacteriophage T4 gene product 5 trimers with histidine tags, cytochrome c, ferritin, heat shock protein, hemoglobin, HSA, and mosaic virus proteins.[175,318–323] The as-prepared nanomaterials are biocompatible and have been used widely, such as in biosensing, bioimaging, cancer therapy, and catalysis. Lysozyme has also been employed in the direct synthesis of metal nanoparticles, including gold and silver nanoparticles in the solution phase.[171,322,324–327]

2.2.1 Au

Synthetic protocols. As shown in Fig. 11, lysozyme protected Au nanoparticles can be synthesized *via* wet chemistry approaches. For example, Li's group developed a facile way to synthesize lysozyme monolayer protected Au nanoparticles by reducing $HAuCl_4$ with $NaBH_4$ in the presence of lysozyme (Fig. 11A and 13A).[171] The as-prepared Au nanoparticles had a size of 2.4 nm. Hydrodynamic size measurements indicated that a monolayer of lysozyme was assembled onto the Au core.[171] Around 15–20 nm Au nanoparticles could be obtained simply by heating the mixture of $HAuCl_4$ and lysozyme (Fig. 11B).[322,326] Because no extra reducing agents were introduced, the protein itself should act as a reducing agent. When a kitchen microwave oven was employed for synthesis (Fig. 11C), the reaction time was shortened to 2 min. Larger Au nanoparticles with a size of 34.5 nm were obtained.[325] Microwave overheating may actually denature the lysozyme used and liberate free cysteines to stabilize the Au nanoparticles.[325]

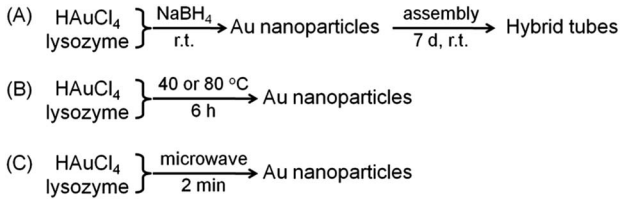

Fig. 11 Synthetic protocols for Au nanoparticles with lysozyme in aqueous solutions.

Mechanism. Understanding the interactions between lysozyme and the Au nanoparticle core as well as the potential conformational changes to lysozyme induced by nanoparticle formation are critical to elucidating the mechanism. Surface-enhanced Raman scattering (SERS) was used by Das *et al.* to investigate the mechanism of lysozyme-capped Au nanoparticles (synthesized as shown in Fig. 11B at 40 °C).[326] As the lysozyme was in the proximity of the Au nanoparticles core, enhanced Raman signals from lysozyme could be probed. The characteristic peaks at 1484, 1545 and 1583 cm^{-1}, corresponding to phenylalanine, tyrosine, tryptophan, and histidine residues, were observed, suggesting the stabilizing roles of these residues (Fig. 12). The presence of a peak at 1289 cm^{-1}, which was assigned to the amide III band, confirmed the assembly of the lysozyme monolayer onto the Au nanoparticles.[326] Note that the IR spectra also showed the presence of amide I, amide II and amide III bonds. Interestingly, although the protein was partially denatured, a peak for S–S bonds at 509 cm^{-1} was observed, indicating that the disulfide bonds remained intact.[326]

Self-assembly. Li and co-workers later serendipitously found that the lysozyme stabilized Au nanoparticles self-assembled into microtubes when they were aged for one week under ambient conditions (Fig. 13B).[171,324] The tubes had a diameter of 1–2 μm with Au nanoparticles decorated onto them. They suggested that hydrogen bonding originating from the amino acid residues of lysozyme may mediate the assembly.[324]

Cellular study. At concentrations as high as 200 μg mL^{-1}, Au nanoparticle capped by lysozyme showed no detectable

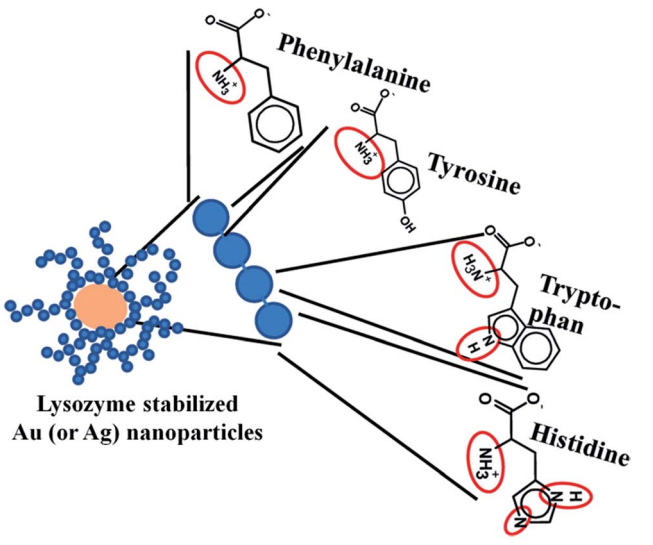

Fig. 12 SERS was adopted to elucidate the mechanism of lysozyme-capped Au and Ag nanoparticles. Certain amino acids played critical roles in stabilizing the nanoparticles. Reprinted with permission from ref. 326, copyright (2009) American Chemical Society.

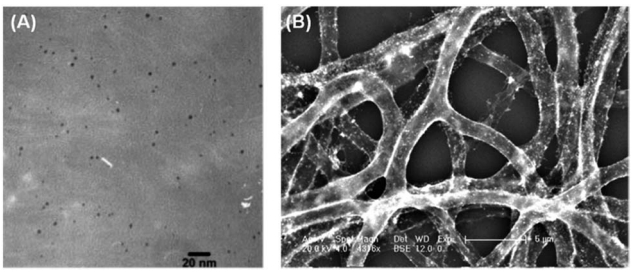

Fig. 13 Lysozyme monolayer-stabilized Au nanoparticles (A) and their self-assemblies into hybrid tubes (B). Reprinted with permission from ref. 171, copyright (2007) American Chemical Society (A); and ref. 324, copyright (2011) American Chemical Society (B).

cytotoxicity, which was evaluated by MTT assay, demonstrating their excellent biocompatibility.[325] After uptake by mouse embryonic fibroblast NIH-3T3 cells, the nanoparticles were accumulated in both cytoplasm and nucleus. The inhibition studies revealed that the Au nanoparticles were taken up by receptor-mediated endocytosis, specifically, the clathrin-dependent endocytosis.[325]

2.2.2 Ag

Synthetic protocols. As discussed above (Fig. 12), lysozyme stabilized Ag nanoparticles were also synthesized *via* the wet chemistry approach.[325] SERS analysis showed that several key amino acid residues, such as phenylalanine, tyrosine, tryptophan, and histidine residues, were involved in interacting with the Ag nanoparticle core. In particular, the Ag–N bonding peak at 236 cm^{-1} was observed, suggesting the potential coordination with Ag nanoparticles *via* nitrogen atoms in the amino acid residues.[325]

An interesting lysozyme catalytic method to prepare Ag nanoparticles was reported.[328] When a mixture of lysozyme and silver acetate in methanol was exposed to light, Ag nanoparticles were formed after about 1 hour exposure. Note, no colloid stable Ag nanoparticles formed in the aqueous solutions. By controlling the silver acetate to lysozyme molar ratios, more monodispersed Ag nanoparticles, 8 nm in size, were obtained. The as-prepared Ag nanoparticles in methanol were transferred successfully into aqueous solution by solvent exchange with dialysis. The Ag nanoparticles in the aqueous solution exhibited as much as 6 months storage stability.[328] The IR spectra indicated the presence of lysozyme in the Ag nanoparticles aqueous solution, even after dialysis, and DLS confirmed the presence of a lysozyme monolayer on the Ag nanoparticle core.[328]

Antimicrobial activity. The hydrolysis of a synthetic substrate mimic indicated that the lysozyme after Ag nanoparticle formation retained its activity as a hydrolase.[328] The antimicrobial activity of the lysozyme-stabilized Ag nanoparticles was evaluated. Remarkably, they inhibited the growth of several bacterial and fungal strains, such as *E. coli*, *S. aureus*, *B. anthracis*, and *C. albicans*. More strikingly, they even exhibited significant antimicrobial activity against *P. mirabilis strains* (LST149 and LST 169A) and *a recombinant E. coli strain* (J53/pMG101), which are usually antibiotic- and silver-resistant.[328] The toxicity towards mammalian cells was also tested, showing that the Ag nanoparticles were nontoxic at the antimicrobial concentrations. The Ag nanoparticles may find wider applications as aseptic materials and therapeutics in the future.

2.3 Other nanomaterials

Many other nanomaterials, including calcium carbonate, metal oxides, metal sulfides, metal tellurides, and composites, have been synthesized using lysozyme.[160,161,163,165,170,329–340]

2.3.1 $CaCO_3$.

Calcium carbonate ($CaCO_3$), one of the major biogenic minerals, is found widely in the exoskeletons and tissues of biomineralizing organisms, providing them with unique mechanical strength and well-defined shapes and structures.[330,331] Avian eggshells are excellent examples of biogenic minerals with hierarchically assembled porous structures, consisting of $CaCO_3$ and biomacromolecules. In an eggshell, $CaCO_3$ exists in the anhydrous form of crystalline calcite, the most thermodynamically stable form.[330] Despite the extensive efforts devoted to understanding the formation mechanism of eggshells, it still remains elusive due to the complexity of the structure. Many studies suggested that lysozyme, one of the key egg white proteins (~3.5%), plays a pivotal role in the calcification of eggshell.[329–333] Lysozyme-mediated $CaCO_3$ *in vitro* biomineralization has been investigated by several groups.

The kinetics and time-dependent morphologies were examined to understand the effects of lysozyme on the precipitation of $CaCO_3$. The results showed that lysozyme could promote the nucleation of $CaCO_3$ while the waiting time for precipitation was prolonged in the presence of lysozyme. Interestingly, the presence of lysozyme affected the habit (*i.e.*, the external shape) of the calcite crystals formed. Without lysozyme, the calcite crystals exhibited a rhombohedral morphology. At lower

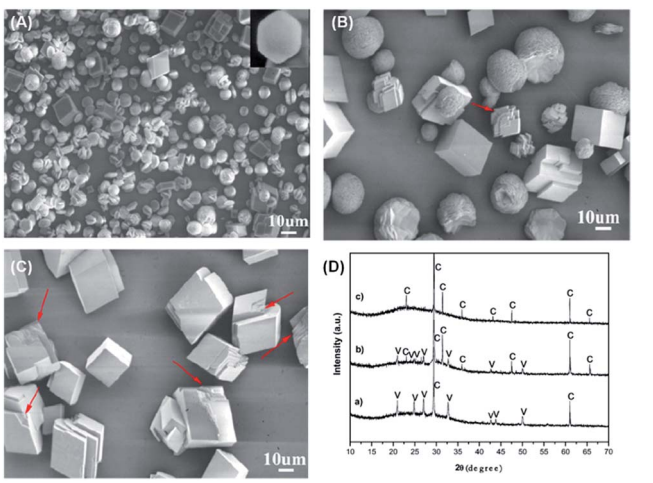

Fig. 14 Lysozyme-mediated calcium carbonate biomineralization. SEM images of $CaCO_3$ formed after 12 h in the absence (A) and presence of 0.5 g L^{-1} lysozyme (B) and 2 g L^{-1} lysozyme (C). (D) Corresponding X-ray powder diffraction patterns of the formed $CaCO_3$. Reprinted with permission from ref. 330, copyright (2009) Elsevier.

concentrations of lysozyme, the rhombohedra morphology was still dominant. At intermediate and higher concentrations of lysozyme, the rhombohedral morphology was converted to calcite with {110}, {100}, and {104} facets, and finally to spherical calcite aggregates, due to the sequentially inhibiting growth of {110}, {100}, and {001} facets.[333]

Usually, the final crystalline calcite is transformed from an intermediate form of $CaCO_3$ by dissolving and recrystallizing the intermediate. Previous studies indicated that adsorbed lysozyme may attract and concentrate calcium ions and provide local nucleation sites. Such interactions between lysozyme and $CaCO_3$ favoured nucleation and led to smaller but more interconnected amorphous $CaCO_3$ compared to the lysozyme-free system.[330,331,333] Lu *et al.* investigated the lysozyme mediated $CaCO_3$ biomineralization by diffusion growth of $(NH_4)_2CO_3$ vapour into $CaCl_2$ aqueous solution. Scanning electron microscopy (SEM) and X-ray diffraction (XRD) clearly revealed the transformation from hexagonal and spherical vaterite (the most unstable form of $CaCO_3$) into coexistent calcite and vaterite, and finally into pure calcite, demonstrating the directing role of lysozyme in the formation of biomineralized $CaCO_3$ (Fig. 14).[330]

2.3.2 Oxides

Silica. Silica (SiO_2) nanoparticles can be prepared by the hydrolysis of precursors, such as tetramethyloxysilane (TMOS), tetraethyloxysilane (TEOS) and their analogues.[341–343] The hydrolysis can be catalysed and tuned by acids, bases, and other catalysts. Researchers have established that lysozyme could assist the hydrolysis reactions for forming silica particles.[161,165,334,344–347] Johnson *et al.* showed that lysozyme could template and significantly accelerate the precipitation of silica *via* a catalytic biomineralization approach (Fig. 15A).[334,344] A minimal concentration of lysozyme was needed for visible silica formation. Moreover, the formation rate and yield of the silica particles could be tuned by changing the amount of lysozyme used. When a higher concentration of lysozyme was used, a higher rate and yield were obtained.[334,344] They also found that the lysozyme still retained its antimicrobial activity (such as lysis of the cell wall of *M. lysodeikticus*), even though it was physically embedded within the silica matrix. The thermal stability was enhanced compared to the free lysozyme.[334] Interestingly, SEM and TEM suggested the silica particles had a hierarchical architecture, *i.e.*, spherical particles of 8–10 nm self-assembled into large particles of 460 nm (Fig. 15A and B). The large particles were mainly spherical in shape, even though other shapes, such as ellipsoid and polyhedral structures, were also observed. To further elucidate the precise interactions of lysozyme and silica matrix, small angle neutron scattering (SANS) with contrast matching technique was employed. As shown in Fig. 15B, the SANS data revealed that the primary building blocks of the final hierarchical architecture were the assembled clusters (3.3 and 8.5 nm) from lysozyme (1.8 nm) and silica nanoparticles (1.3 nm). The primary building blocks then aggregated together to form final silica particles as large as 460 nm.[334]

Interestingly, the reaction conditions (such as stirring *versus* sonication) played key roles in controlling the morphology of the silica in the presence of lysozyme.[165,346,347] The hydrolysis reaction with stirring produced granular silica particles. However, when sonication was applied, hollow spherical particles of 0.5–15 μm with a shell thickness of 100 nm were formed.[165,346,347] As proposed by Sakaguchi *et al.*, the hollow structures were formed *via* the following mechanism. First, sonication would induce the formation of TEOS emulsion droplets, which was covered with lysozyme. The lysozyme would then catalyze hydrolysis *in situ* and form lysozyme-silica shell structures. The TEOS leaked from the droplets would be catalytically hydrolyzed further by lysozyme, which resulted in an increase in particle shell thickness. When the lysozyme used is insufficient, sonication would decrease the droplet size and thus the final silica size. On the other hand, when excess lysozyme molecules are present, the single particles would grow together and form aggregates or sponge-like structures.[165] Further post-treatment of the hollow silica structures by calcination would produce either mesoporous silica (500 °C) or cage-like hollow silica spheres (700 °C).[346]

Titania. The lysozyme-catalyzed hydrolysis of the corresponding precursors, such as potassium hexafluorotitanate (PHF-Ti) and titanium(IV) bis(ammonium lactato)dihydroxide (Ti-BALDH), provides a rapid and facile method to fabricate titania (TiO_2) particles under ambient conditions.[161] The lysozyme molecules were entrapped simultaneously within the titania matrix during the hydrolysis reaction. The entrapped lysozymes retained their antimicrobial activities. Additional enzymes could also be co-entrapped. For example, butyrylcholinesterase was encapsulated within the titania/lysozyme hybrids during titania precipitation and retained its enzymatic activity. Moreover, the encapsulated enzymes exhibited enhanced thermal stability compared to the free ones. For both titania particles from PHF-Ti and Ti-BALDH, selected area electron diffraction (SAED) and XRD confirmed that they were amorphous. Interestingly, different precursors would produce titania with different sizes, compositions and morphologies. For example, titania from PHF-Ti gave polydispersed particles with a size of 100 nm to 1 μm, whereas titania from Ti-BALDH produced fine particles, 10–50 nm in size. In addition, the latter had a higher lysozyme content than the one from PHF-Ti. The slightly lower activity of the entrapped lysozymes compared to the free ones was attributed to physical steric hindrance after entrapment.[161]

When examining the interactions of lysozyme and prepared titania nanoparticles, 60 nm in size, Gao *et al.* found that the titania nanoparticles affected the enzymatic activities of lysozyme (Fig. 15C). Based on detailed studies, a two-step binding mode was proposed to interpret the phenomenon. The negatively-charged titania nanoparticles interacted with the positively-charged lysozymes electrostatically first. After the initial binding, the proximity of lysozymes to the surface of the titania nanoparticles would induce the formation of new hydrogen bonds (such as N–H···O and O–H···O) (Fig. 15D). Such bridges between the titania nanoparticles and lysozyme monolayers would induce local deformation of the absorbed lysozymes and decrease the enzymatic activity, as observed.[160]

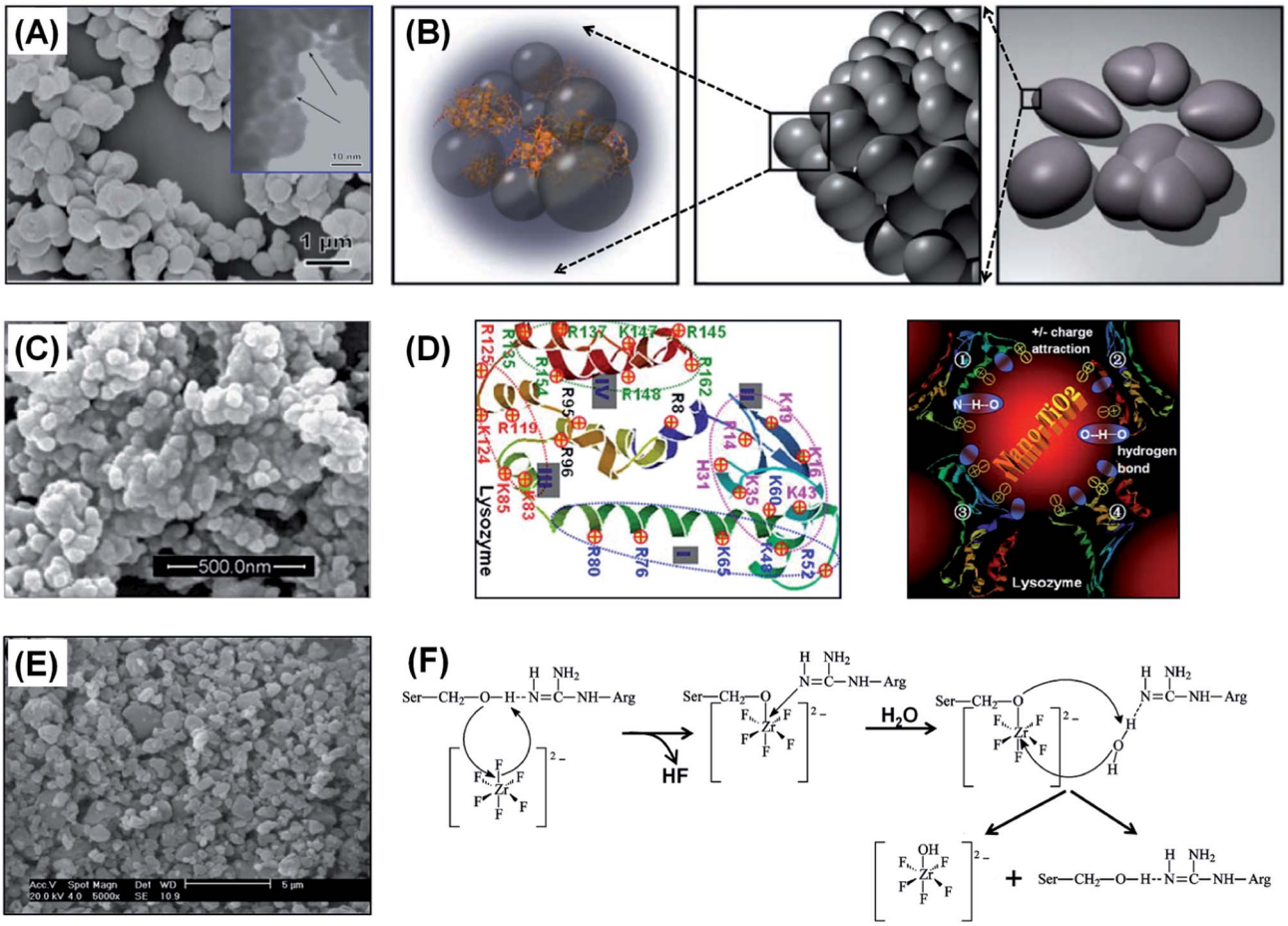

Fig. 15 Lysozyme-directed approaches to oxides. (A) SEM and TEM (inset) images of silica formed by the hydrolysis of TMOS; (B) schematic diagram of the hierarchical assembly of the silica particles; (C) SEM image of titania-lysozyme nanoparticles; (D) proposed interactions of lysozyme and the titania nanoparticles; (E) SEM image of zirconia formed by the hydrolysis of K_2ZrF_6; (F) proposed mechanism of lysozyme-directed forming zirconia. Reprinted with permission from ref. 334, copyright (2010) John Wiley and Sons (A and B); ref. 160, copyright (2009) Springer (C and D); and ref. 335, copyright (2008) American Chemical Society (E and F).

Zirconia. Zirconia (ZrO_2) particles were prepared by the catalytic hydrolysis of K_2ZrF_6 in the presence of lysozyme at room temperature.[335] Irregular particles with a size of 1 μm rather than small nanoparticles were obtained, probably due to rapid hydrolysis catalyzed by lysozyme (Fig. 15E). Careful characterization with energy-dispersive X-ray spectrometry (EDX), thermogravimetric analysis (TGA), IR and XPS, confirmed the formation of zirconia particles. Interestingly, thermally denatured lysozyme could also catalyze hydrolysis, indicating that some amino acid residues of the side chains (rather than the residues of the active site) were responsible for the lytic reaction (Fig. 15F). Moreover, when other enzymes, such as yeast alcohol dehydrogenase (YADH), were introduced to the reaction precursor solution of lysozyme and K_2ZrF_6, the enzymes could be incorporated in the zirconia particles. The incorporated enzymes exhibited enhanced thermal and pH stability.[335]

2.3.3 Metal sulfides and tellurides. Several metal sulfides stabilized by lysozyme were synthesized by Qin *et al.*[336–338] Cubic zinc blende phase of ZnS nanoparticles with a spherical shape were prepared using zinc acetate and thioacetamide as precursors in the presence of an aqueous lysozyme solution. The ZnS particles had an average size of around 40 nm. The IR spectra suggested that the –OH and –NH groups of lysozyme may be involved in interacting with the ZnS nanoparticles.[336] Using a similar approach, cubic PbS nanoparticles with a mean size of 45 nm were also synthesized. Interestingly, the photoluminescence spectrum centred at 470 nm was obtained, which probably originated from sulphur vacancy defects.[337] Photoluminescence tuneable HgS nanoparticles could also be obtained by changing the ratio of lysozyme to the precursors used. Smaller HgS nanoparticles with stronger photoluminescence were obtained at higher lysozyme concentrations (*i.e.*, HgS nanoparticles with an average size of 14, 19, and 27 nm were obtained with 5, 3, and 1 mg mL^{-1} lysozyme, respectively).[338] Gao and co-workers showed that single-crystalline bismuth sulfide and bismuth oxide nanowires with lengths in the micrometer range could be fabricated under mild conditions by using a lysozyme-assisted approach. Bismuth sulfide nanowires had diameters of 10–50 nm, whereas bismuth oxide had an average diameter of 8 nm. Coordination between Bi^{3+} and certain groups of lysozyme may play a key role in directing

the formation of nanowires rather than other irregular shapes.[348]

Using the evaporation-induced self-assembly method, microscale dendrite structures were fabricated from a mixture of thioglycolic acid capped CdTe quantum dots (~2.3 nm) and different proteins (including lysozyme) on glass substrates. The dendrite structures could be fine-tuned by controlling the pH of the reaction solution and by introducing metal ions.[163]

2.3.4 Composites. Nanocomposites are nanomaterials with multiple components, which are usually effectively integrated. Compared with mono-component nanomaterials, nanocomposites may have enhanced properties due to synergistic effects. Liu *et al.* showed that ternary TiO_2–SiO_2–Ag nanocomposites indeed exhibited enhanced visible-light photocatalytic activity towards Rhodamine B degradation.[170] The nanocomposites were prepared in a step-wise manner *via* a facile lysozyme-directed approach (Fig. 16). Specifically, TiO_2 nanoparticles of ~280 nm were first formed by the lysozyme-induced hydrolysis of Ti-BALDH. It was suggested that the positively charged arginine and lysine residues of lysozyme interacted with Ti-BALDH electrostatically and induced hydrolysis. The TiO_2–SiO_2 composites were then obtained by forming SiO_2 patch layers from sodium silicate onto the surface of the as-prepared TiO_2 nanoparticles. Finally, Ag nanoparticles of ~25 nm were produced *in situ* and deposited on the TiO_2–SiO_2 composites by reduction of Ag^+ with the reducing residues of lysozyme (such as tryptophan, tyrosine, phenylalanine, and histidine residues). The formation of TiO_2–SiO_2–Ag nanocomposites was confirmed by EDX elemental mapping and TEM imaging as well as other characterization techniques. Owing to the synergistic effects of the enhanced light harvesting from plasmonic Ag nanoparticles and increased adsorption capacity of dyes (Rhodamine B here) from SiO_2, the highest degradation rate of 0.841 h^{-1} was observed for the TiO_2–SiO_2–Ag nanocomposites. For comparison, the rates for TiO_2, TiO_2–SiO_2, and TiO_2–Ag nanomaterials were 0.098 h^{-1}, 0.448 h^{-1}, and 0.330 h^{-1}, respectively. The ternary nanocomposites could be recycled because of the strong chemical stability.[170]

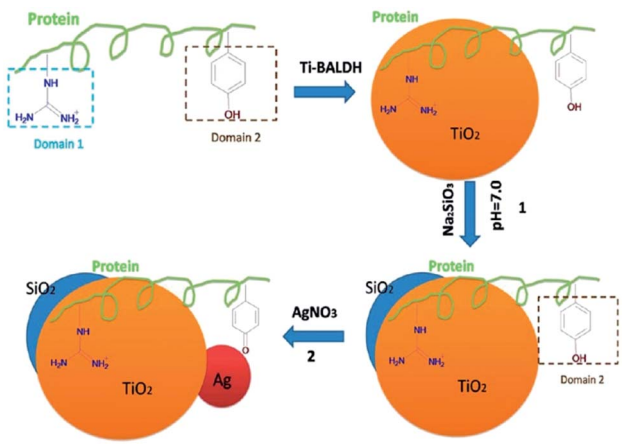

Fig. 16 Lysozyme was used to direct the synthesis of the TiO_2–SiO_2–Ag nanocomposites. Reprinted with permission from ref. 170, copyright (2013) American Chemical Society.

3. Lysozyme crystals

Although protein crystals, especially protein single crystals, are traditionally grown to obtain structural information in molecular biology, researchers have established that they can be regarded as novel porous materials.[10,108,110,114,157,159,162,164,169,189,190,349–355] When treated as emerging materials, protein crystals have several unique features compared to other materials and their assemblies.[10,108,114,157,159,162,164,169,189,190,349–354,356–360] First, they have highly ordered 3D structures assembled periodically from the corresponding protein monomers. Second, they are porous materials with precisely controlled pore sizes. The pores are usually filled with solvents, such as aqueous buffer solutions. These solvent channels can be used as templates to grow nanomaterials and encapsulate guest molecules. Third, the amino acid residues exposed to the solvent channels can interact with incoming species (such as coordinating with the added metal ions), which in turn may direct and tune the formation of designed materials. Fourth, the formed materials (or encapsulated guest molecules) in the porous channels and the host protein crystals have synergic effects, rendering hybrid materials with enhanced or even new properties. Fifth, the single crystals of proteins may provide atomic resolution structural information and help understand the mechanisms involved. Although protein crystals are inherently fragile and the growth of protein crystals is normally quite challenging, the controllable manipulation of protein crystals is now achievable thanks to the substantial progress in the field of protein crystal engineering.[108,189,190] Recently, rapid progress has been made in directing the synthesis of functional nanomaterials with protein crystals.

In this section, the use of lysozyme crystals (in both cross-linked and intact native forms) to direct the synthesis of different kinds of hybrid nanomaterials is discussed.

3.1 Metal nanomaterials

3.1.1 Au. Mann *et al.* reported the synthesis of plasmonic metal nanomaterials within cross-linked lysozyme crystals.[114] The cross-linked lysozyme crystals were obtained by soaking the native lysozyme single crystals in the crystallization buffer solution containing glutaraldehyde. Arrays of plasmonic Au nanofilaments were then obtained by sequestrating $HAuCl_4$ into the cross-linked lysozyme crystals, followed by *in situ* reduction with $NaBH_4$. The formation of plasmonic Au nanostructures could be followed easily by a colour change of the crystals (Fig. 17). Diffuse reflectance UV-visible spectroscopic measurements revealed two absorbance peaks centred at around 583 and 684 nm, confirming the formation of plasmonic Au nanostructures. The two peaks were assigned to the transverse and longitudinal plasmon resonance bands, respectively. TEM further confirmed the formation of Au nanofilaments infiltrated within the porous channels of the cross-linked lysozyme crystals. The IR spectra indicated that the presence of Au

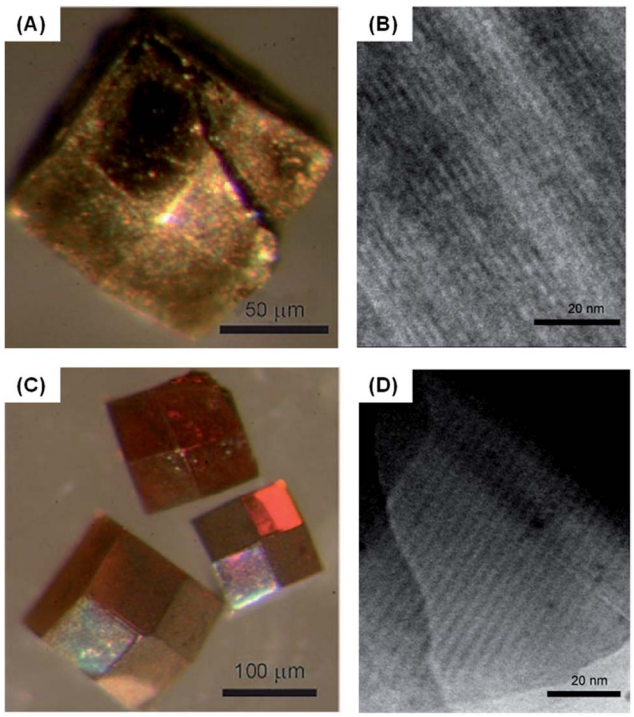

Fig. 17 Cross-linked lysozyme crystals were used to direct the synthesis of plasmonic metal nanostructures. Optical and corresponding TEM images of the Au nanostructures-doped cross-linked lysozyme crystals (A and B) and Ag nanostructures-doped cross-linked lysozyme crystals (C and D). Reprinted with permission from ref. 114, copyright (2010) John Wiley and Sons.

nanostructures did not affect the protein structures significantly. Although the tetragonal morphology of the crystals remained effectively unchanged after the formation of Au nanostructures, some crystals were cracked (Fig. 17). Single crystal X-ray diffraction showed that the hybrid crystals only exhibited low intensity reflections, which was probably associated with a disordered tetragonal phase.[114]

Later, they performed a more detailed study to investigate the optical response of the infiltrated Au nanostructures within the cross-linked lysozyme crystals. Using angle- and polarization-dependent spectroscopy, they showed that the encapsulated Au nanostructures were isolated with spheroidal or slightly anisotropic shapes.[354] No continuous nanowires were detected inside the crystal host. The plasmonic response was attributed to the isolated Au nanostructures. Interestingly, fluorescent measurements suggested the presence of ultrasmall Au clusters, which emitted light at around 650–750 nm.[354] The simultaneous formation of both plasmonic and fluorescent Au nanostructures with cross-linked lysozyme crystals may provide a new approach to the synthesis of multi-functional materials.

As mentioned above, the cross-linking and the post-growth of Au nanostructures may cause distortions or even damage to the single crystal structure of lysozymes. In addition, the formation of Au nanostructures *via* chemical reduction was relatively fast, making it quite challenging to perform kinetic studies. To address these issues, Wei *et al.* developed a novel strategy for the *in situ* growth of Au nanoparticles within intact single crystals of lysozyme for the first time (Fig. 18).[159] Starting with $ClAuS(CH_2CH_2OH)_2$ (referred to Au(I)) as the precursor, they could controllably grow Au nanoparticles without using any reducing reagents due to the disproportionation chemistry of Au(I). The formation of Au nanoparticles was slowed down due to the semi-solid nature of the protein crystals, making the system amenable to detailed kinetic and mechanism studies. On the other hand, the remaining intact single crystals enabled careful structural characterization by X-ray crystallography. The time-dependent growth of Au nanoparticles within the lysozyme single crystals was monitored by the colour change of the crystals and further confirmed by quantitative analysis of the Au nanoparticle sizes by TEM. This clearly showed the gradual growth of Au nanoparticles within the crystals over time. In addition, the 3D distribution of Au nanoparticles within lysozyme crystals was determined by STEM with tomography, validating the encapsulation of Au nanoparticles inside the crystals. More, atomic resolution X-ray crystal structures were obtained. Careful analysis of the crystal structures indicated that certain amino acid residues, such as histidine, played critical roles in directing the growth of Au nanoparticles.[159] This also suggested that the growth of Au nanoparticles within lysozyme crystals was a dynamic process that may involve metal ions transfer, which was supported by later studies.[120,309] The developed strategy was also applicable to other systems, such as the thaumatin protein.[159]

Wei and co-workers also developed an effective way to fine tune the growth of Au nanoparticles within the lysozyme single crystals.[159] When using Hg^{2+} ions as an additive, the growth rate was accelerated significantly (Fig. 19). Surprisingly, many other divalent metal ions tested did not show such an accelerating effect. This was probably due to the highly specific Ag^{+}–Hg^{2+} metallophilic interaction. When tris(2-carboxyethyl)phosphine (TCEP) was added as an additive, the growth rate was inhibited. The inhibitory effect of TCEP could have been caused by the stronger interaction between Au(I) and TCEP. Other molecules, such as histidine, could also be used as inhibitors.[159]

Owing to the excellent catalytic properties of gold nanomaterials, the catalytic performance of the Au nanoparticles within lysozyme single crystals was also evaluated by Wei *et al.*[10] Using the reduction of *p*-nitrophenol to *p*-aminophenol by $NaBH_4$ as a model reaction, they showed that the catalytic

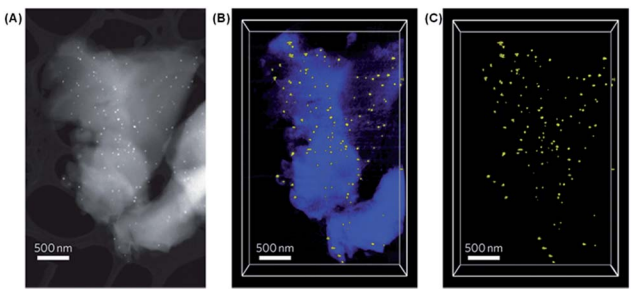

Fig. 18 Protein-directed growth of gold nanoparticles within a single crystal of lysozyme. Reprinted with permission from ref. 159, copyright (2011) Nature Publishing Group.

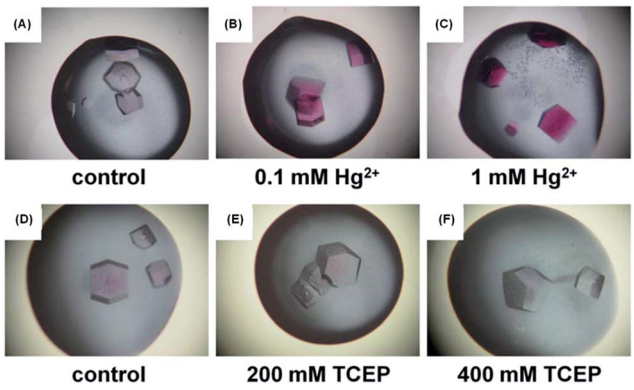

Fig. 19 Fine tuning growth of gold nanoparticles within a single crystal of lysozyme. (A–C) accelerating the growth rate by using Hg^{2+} as an additive; (D and E) decelerating the rate of the growth by using TCEP as an additive. Reprinted with permission from ref. 159, copyright (2011) Nature Publishing Group.

activities of the Au nanoparticles could be tuned precisely by controlling the growth (thus the size) of Au nanoparticles (Fig. 20). The relationship between catalytic activity of the Au nanoparticles and their size was elucidated. The catalytic activity of the Au nanoparticles initially increased with the increase of nanoparticle size until the size reached 7.4 nm, after which the activity decreased with increasing nanoparticle size.[10] In addition, additives, such as Hg^{2+} and TCEP, could be used to fine tune the catalytic activities by controlling the growth of Au nanoparticles. To efficiently recycle the catalysts, the Au nanoparticle-embedded crystals were post cross-linked with glutaraldehyde.[10]

Liang *et al.* employed a slightly different approach to the synthesis of Au nanoparticles within cross-linked lysozyme crystals.[352] The cross-linked lysozyme crystals were also obtained with glutaraldehyde. $HAuCl_4$ was then sequestrated into the crystals by soaking the crystals in a $HAuCl_4$ solution.

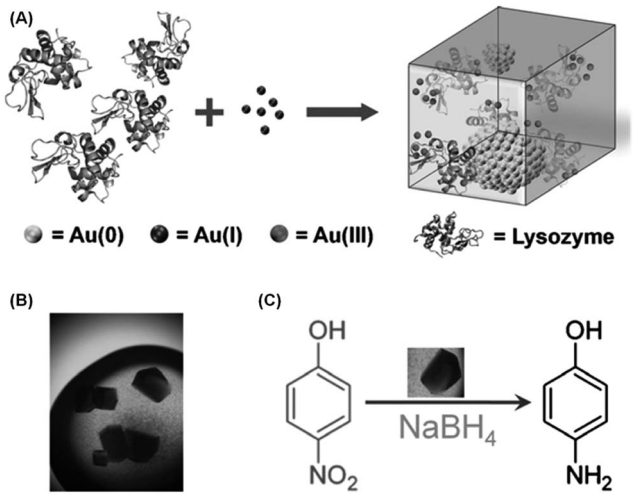

Fig. 20 Catalysis of gold nanoparticles within a lysozyme single crystal. Reprinted with permission from ref. 10, copyright (2012) John Wiley and Sons.

Instead of adding $NaBH_4$ for reduction, NaOH was added to the $HAuCl_4$-soaked crystals at 37 °C for reduction. As discussed above (Section 2.1.1), $HAuCl_4$ could be reduced to Au^0 by certain amino acid residues of lysozyme under basic conditions. The as-prepared Au nanoparticles had an average size of 2.2 nm. This further showed that the Au nanoparticles exhibited high activity towards the catalytic reduction of *p*-nitrophenol to *p*-aminophenol by $NaBH_4$. Moreover, the Au nanoparticle-doped crystals could be recycled and reused more than 20 times, showing great potential for practical applications.[352]

3.1.2 Ag. The synthesis of Ag nanostructures within cross-linked lysozyme crystals were also reported by Mann and co-workers.[114] Instead of using a chemical reducing reagent, UV light was applied to reduce the sequestrated silver ions within the cross-linked lysozyme crystals. The formation of Ag nanostructures after *in situ* photoreduction was also followed by a colour change in the crystals, which was further confirmed by TEM (Fig. 17). The formed Ag nanostructures were also isolated instead of forming continuous nanowires.[354] The transverse and longitudinal plasmonic peaks corresponding to the formed Ag nanostructures were observed at around 412 and 505 nm, respectively.[114] Although the Ag nanostructures-doped crystals exhibited a more intact tetragonal morphology than the Au nanostructures-doped ones, the X-ray diffraction patterns deteriorated progressively with increasing UV irradiation time. These results indicated that the proposed methods for the synthesis of metal nanostructures could cause structural distortion or even damage to the crystal host.

Adopting a similar approach, Ag nanoparticles within cross-linked lysozyme crystals were prepared by Liang and co-workers. The Ag nanoparticles were obtained by the reduction of sequestrated $AgNO_3$ with $NaBH_4$.[351] The catalytic reduction of *p*-nitrophenol to *p*-aminophenol by $NaBH_4$ was also demonstrated.

3.2 Others

3.2.1 Quantum dots. Recently, fluorescent semiconductor quantum dots were fabricated within intact single crystals of lysozyme (Fig. 21).[162] CdS quantum dots with red fluorescence were synthesized within single crystals of lysozyme using an *in situ* growth approach. Interestingly, the CdS quantum dots within the crystals emitted much stronger fluorescence compared to those without protein crystals. These results suggest that the protein crystals may provide a unique micro-environment for encapsulated CdS quantum dots with enhanced fluorescence. In addition, the fluorescence was tuneable, and could be enhanced by the addition of Ag^+ and quenched by Hg^{2+}.[162] The X-ray crystallographic data showed that several amino acid residues, including histidine, participated in the direct formation of CdS quantum dots.

3.2.2 Magnetic nanoparticles. The protein crystalline lattice and the sizes and morphologies of the pores in porous protein crystals can be tuned by controlling the crystallization conditions. By exploring this property, Abe *et al.* synthesized CoPt nanoparticles with different sizes and compositions within the cross-linked lysozyme crystals (Fig. 22).[169]

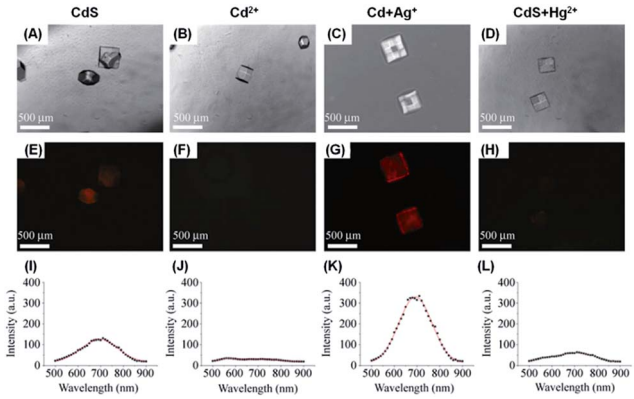

Fig. 21 Red fluorescent CdS quantum dots were formed within lysozyme single crystals and the fluorescent properties could be fine-tuned by external chemical stimuli. Bright field (A–D), fluorescence images (E–H), and emission spectra (I–L) of lysozyme single crystals. Reprinted with permission from ref. 162, copyright (2013) Tsinghua University Press and Springer.

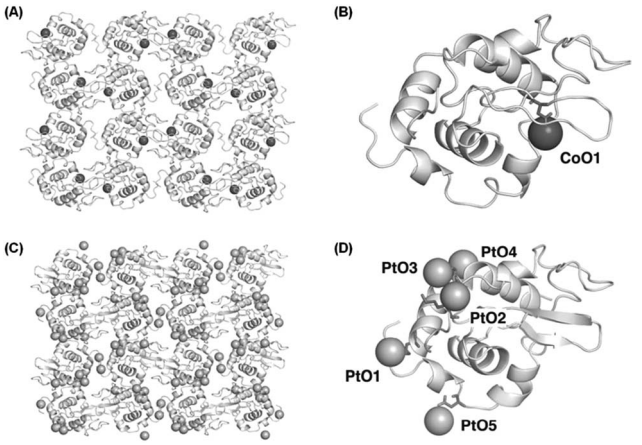

Fig. 23 Crystal lattice and molecular structures of a cross-linked orthorhombic lysozyme crystal containing Co^{2+} ions (A and B) and Pt^{2+} ions (C and D). Reprinted with permission from ref. 169, copyright (2012) John Wiley and Sons.

Orthorhombic, tetragonal, and monoclinic lysozyme crystals were grown with corresponding crystallization buffers. The crystals were then cross-linked with glutaraldehyde to maintain the lattice structures. After soaking the cross-linked crystals in the buffer solutions containing $CoCl_2$ and K_2PtCl_4, the CoPt nanoparticles were formed *in situ* by chemically reducing the as-soaked Co^{2+} and Pt^{2+} with $NaBH_4$. TEM clearly showed that the sizes of the CoPt nanoparticles were dependent on the pore sizes of the crystals, *i.e.*, large pores could template the formation of large nanoparticles while small pores led to the formation of small nanoparticles (Fig. 22).[169] CoPt is among the magnetic materials with high magnetocrystalline anisotropy. Therefore, their magnetic properties were investigated using a superconducting quantum interference device magnetometer.

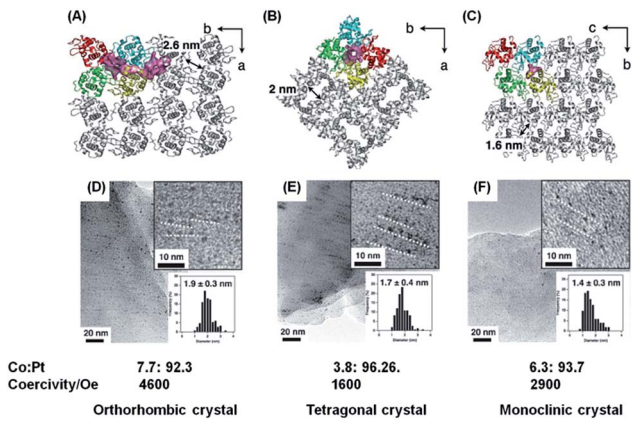

Fig. 22 Porous protein crystals as reaction vessels for controlling the magnetic properties of CoPt nanoparticles. (A–C) crystal lattice structures of different lysozyme crystals; (D and E) TEM images of CoPt nanoparticles formed in the corresponding cross-linked lysozyme crystals. The Co to Pt ratios and coercivity of the formed CoPt nanoparticles are also listed. Reprinted with permission from ref. 169, copyright (2012) John Wiley and Sons.

The order of the CoPt nanoparticles' coercivity followed the content of Co of the nanoparticles instead of the nanoparticle size, which was consistent with a previous report.[169]

The X-ray crystallographic structures were also obtained to further understand the mechanism (Fig. 23).[169] Both Co^{2+} and Pt^{2+} ions were accumulated within the solvent channels of the crystals. For both orthorhombic and tetragonal lysozyme crystals, the ratio of the observed Co to Pt was 1 : 5, suggesting that additional Pt^{2+} ions may be bound randomly to the solvent channels. The crystallographic data suggested that the sizes, compositions, and magnetic properties of the CoPt nanoparticles were affected by the number and position of metal ions accumulated.[169] Metal ion translocation was also suggested, which is consistent with previous results.[159,309]

Interestingly, when the CoPt nanoparticles were synthesized in a lysozyme solution, only aggregates were obtained. The aggregates also showed much lower coercivity than CoPt nanoparticles within the lysozyme crystals.[169] Such results indicated that the microenvironments and unique structures of lysozyme crystals play critical roles in directing the formation of magnetic CoPt nanoparticles.

3.2.3 Polypyrrole nanostructures. Polypyrrole is a conducting polymer with exceptional biocompatibility and conductive properties, but is difficult to process because of its intrinsic brittleness and insolubility. To improve the performance of polypyrrole (such as mechanical and electrical properties), Mann and co-workers developed an interesting strategy to template the synthesis and organization of polypyrrole within the solvent channels of cross-linked lysozyme crystals.[164] Glutaraldehyde was used to cross-link the crystals, as reported previously. The oxidant, ammonium persulfate, was introduced into the channel by soaking. The ammonium persulfate-loaded crystals were then dried and exposed to pyrrole vapour. The partially oxidized polypyrrole was *in situ* formed within the solvent channel after approximately 24 hours exposure. The as-prepared polypyrrole-doped lysozyme crystals were black/brown in colour. TEM imaging revealed the presence of continuous

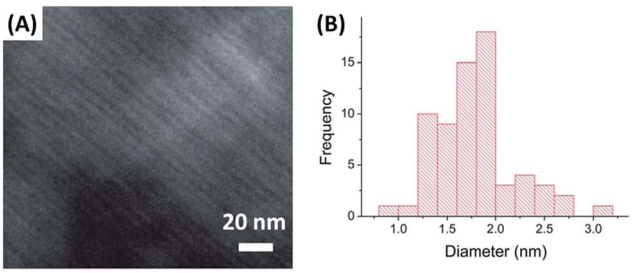

Fig. 24 (A) High resolution TEM image of polypyrrole nanostructures formed within the solvent channels of cross-linked lysozyme crystals. (B) Histogram of the diameters of formed the polypyrrole nanostructures. Reprinted with permission from ref. 164, copyright (2012) Royal Society of Chemistry.

stripes, 1.8 nm in diameter, which was attributed to the formed polypyrrole (Fig. 24). The thickness of the stripes matched well with the width of the solvent channels of the lysozyme crystals, suggesting the successful templating effect of the cross-linked lysozyme crystals. Although the macroscopic tetragonal morphology was preserved after forming polypyrrole, the crystalline lattice of lysozyme was disrupted significantly because no X-ray diffraction patterns were obtained. Compared to undoped lysozyme crystals, the polypyrrole-doped crystals exhibited measurable conductivity (>10^7 Ωm *vs.* 10^4 Ωm). Note that the conducting mechanism remains to be clarified. Moreover, force-displacement measurements by atomic force microscopy revealed that the mechanical plasticity of lysozyme crystals after forming polypyrrole inside was enhanced.[164,361,362] The proposed method may be applicable to other conducting materials, such as polyaniline.[164]

4. Conclusions and perspectives

This *Feature Article* demonstrates that lysozyme is a valuable model protein to develop synthetic methodologies for various functional nanomaterials, to elucidate the formation mechanism and protein–nanomaterial interactions of the nanomaterials, and to explore potential applications (Table S1†).

Based on the above discussions, several key points can be summarized. First, proteins and other biomolecules can be used to rationally design and synthesize functional nanomaterials with the desired properties for wide applications. Second, certain amino acid residues in a protein play critical roles in directing the formation of nanomaterials. Third, the unique microenvironments and structures of protein assemblies, such as protein crystals, also play important roles in directing the synthesis of functional materials. Fourth, a combination of advanced techniques, such as electron microscopy with tomography and X-ray crystallography from different areas, provides a promising opportunity to fully characterize complicated hybrid nanomaterials.

Although substantial progress has been made in the field of protein-directed approaches to functional nanomaterials, several challenges remain to be addressed.

First, great efforts should be focused on understanding the formation mechanism of functional nanomaterials. For example, even for the extensively studied gold nanoclusters, no exact mechanism was proposed until now.[121,155,306,309] It is unclear that how the bound gold ions translocate and form the final clusters among the proteins.[121,155,306,309] On one hand, the ultrasmall size of gold nanoclusters and the presence of a protein matrix make it very challenging to obtain structural information by TEM imaging. On the other hand, the gold core also affects the MS characterization.[120] High-resolution STEM with tomography, such as STEM with a subatomic resolution, may be an alternative approach to obtain structural information. X-ray crystallography should be another rewarding choice but it is usually very time-consuming.[207] Studies in the gas phase will also provide valuable clues and insights to understanding the reaction mechanism in the solution phase.[311,316] The theoretical simulation should not be overlooked because it would be able to predict the structural information when combined with the experimental results.

Second, the scopes of the nanomaterials fabricated should be explored further. The majority of metal nanomaterials discussed above were noble metal materials. It will be interesting to synthesize other metal materials, such as transition metal and rare earth nanomaterials, with proteins. Most of the as-prepared nanomaterials were spherical. Therefore, nanomaterials with other shapes and morphologies should be another focus in future studies. The design and preparation of multiple functional nanomaterials will be another promising field to be investigated.

Third, most of the model proteins used were lysozyme, BSA, ferritin, heat shock protein *etc.*[154,174,363,364] Other proteins, especially those with biofunctionality, should be tested. For example, when the peptide of a small variant of protein A and a Au nanoparticle-directing peptide are placed together *via* recombinant protein engineering, the protein chimera could allow the template synthesis of biofunctionalized Au nanoparticles in a one-pot fashion.[158]

The ultimate goal would be rational *de novo* design and synthesis of personalized functional nanomaterials with the desired structures and properties based on computation in the future.[365,366]

Acknowledgements

We would like to thank the National Natural Science Foundation of China (no. 21405081), the Natural Science Foundation of Jiangsu Province (no. BK20130561 and BK20140593), the 973 Program (no. 2015CB659400), the 985 Program of Nanjing University, the Priority Academic Program Development of Jiangsu Higher Education Institutions (PAPD), the Shuangchuang Program of Jiangsu Province, and the Thousand Talents Program for Young Researchers for financial support. The authors would like to thank Professor Flavio Maran at University of Padova for the insightful discussions.

Notes and references

1 M. Bruchez, M. Moronne, P. Gin, S. Weiss and A. P. Alivisatos, *Science*, 1998, **281**, 2013–2016.

2 A. P. Alivisatos, *Science*, 1996, **271**, 933–937.
3 A. P. Alivisatos, K. P. Johnsson, X. G. Peng, T. E. Wilson, C. J. Loweth, M. P. Bruchez and P. G. Schultz, *Nature*, 1996, **382**, 609–611.
4 P. Alivisatos, *Nat. Biotechnol.*, 2004, **22**, 47–52.
5 W. C. W. Chan and S. M. Nie, *Science*, 1998, **281**, 2016–2018.
6 S. M. Nie and S. R. Emery, *Science*, 1997, **275**, 1102–1106.
7 L. H. Tan, H. Xing and Y. Lu, *Acc. Chem. Res.*, 2014, **47**, 1881–1890.
8 Y. Lu and J. W. Liu, *Acc. Chem. Res.*, 2007, **40**, 315–323.
9 M. Valden, X. Lai and D. W. Goodman, *Science*, 1998, **281**, 1647–1650.
10 H. Wei and Y. Lu, *Chem.–Asian J.*, 2012, **7**, 680–683.
11 A. S. Arico, P. Bruce, B. Scrosati, J. M. Tarascon and W. Van Schalkwijk, *Nat. Mater.*, 2005, **4**, 366–377.
12 T. Rueckes, K. Kim, E. Joselevich, G. Y. Tseng, C. L. Cheung and C. M. Lieber, *Science*, 2000, **289**, 94–97.
13 L. Zhang, H. X. Chang, A. Hirata, H. K. Wu, Q. K. Xue and M. W. Chen, *ACS Nano*, 2013, **7**, 4595–4600.
14 H. Wei, B. L. Li, J. Li, S. J. Dong and E. K. Wang, *Nanotechnology*, 2008, **19**, 095501.
15 R. Elghanian, J. J. Storhoff, R. C. Mucic, R. L. Letsinger and C. A. Mirkin, *Science*, 1997, **277**, 1078–1081.
16 C. M. Niemeyer, *Angew. Chem., Int. Ed.*, 2001, **40**, 4128–4158.
17 E. Katz and I. Willner, *Angew. Chem., Int. Ed.*, 2004, **43**, 6042–6108.
18 M. C. Daniel and D. Astruc, *Chem. Rev.*, 2004, **104**, 293–346.
19 N. L. Rosi and C. A. Mirkin, *Chem. Rev.*, 2005, **105**, 1547–1562.
20 H. Wei, B. L. Li, J. Li, E. K. Wang and S. J. Dong, *Chem. Commun.*, 2007, 3735–3737.
21 Y. Wang, H. Wei, B. Li, W. Ren, S. Guo, S. Dong and E. Wang, *Chem. Commun.*, 2007, 5220–5222.
22 H. Wei, Y. Du, J. Z. Kang and E. K. Wang, *Electrochem. Commun.*, 2007, **9**, 1474–1479.
23 C. L. Guo, Y. H. Song, H. Wei, P. C. Li, L. Wang, L. L. Sun, Y. J. Sun and Z. Li, *Anal. Bioanal. Chem.*, 2007, **389**, 527–532.
24 G. Wei, L. Wang, L. L. Sun, Y. H. Song, Y. J. Sun, C. L. Guo, T. Yang and Z. Li, *J. Phys. Chem. C*, 2007, **111**, 1976–1982.
25 H. Wei and E. Wang, *Anal. Chem.*, 2008, **80**, 2250–2254.
26 H. Wei, C. G. Chen, B. Y. Han and E. K. Wang, *Anal. Chem.*, 2008, **80**, 7051–7055.
27 L. L. Sun, Y. H. Song, L. Wang, C. L. Guo, Y. J. Sun, Z. L. Liu and Z. Li, *J. Phys. Chem. C*, 2008, **112**, 1415–1422.
28 Z. Z. Lv, H. Wei, B. L. Li and E. K. Wang, *Analyst*, 2009, **134**, 1647–1651.
29 F. G. Xu, K. Cui, Y. J. Sun, C. L. Guo, Z. L. Liu, Y. Zhang, Y. Shi and Z. Li, *Talanta*, 2010, **82**, 1845–1852.
30 L. B. Zhang, H. Wei, J. Li, T. Li, D. Li, Y. H. Li and E. K. Wang, *Biosens. Bioelectron.*, 2010, **25**, 1897–1901.
31 Y. Zhang, F. G. Xu, Y. J. Sun, C. L. Guo, K. Cui, Y. Shi, Z. W. Wen and Z. Li, *Chem.–Eur. J.*, 2010, **16**, 9248–9256.
32 Z. L. Liu, B. Zhao, Y. Shi, C. L. Guo, H. B. Yang and Z. Li, *Talanta*, 2010, **81**, 1650–1654.
33 H. Wei and E. K. Wang, *Chem. Soc. Rev.*, 2013, **42**, 6060–6093.
34 S. H. Gao, F. Y. Liu, B. T. Zhang, Y. J. Wang, H. M. Zhang and Z. X. Wang, *Chin. J. Anal. Chem.*, 2013, **41**, 811–816.
35 Q. H. Guo, J. S. Huang and T. Y. You, *Chin. J. Anal. Chem.*, 2013, **41**, 210–214.
36 S. J. Guo and E. K. Wang, *Acc. Chem. Res.*, 2011, **44**, 491–500.
37 C. X. Li, J. Adamcik and R. Mezzenga, *Nat. Nanotechnol.*, 2012, **7**, 421–427.
38 Y. A. Yuan, X. X. He, H. Shi, K. M. Wang, X. Wu and X. Q. Huo, *Chem. J. Chin. Univ.*, 2010, **31**, 2167–2172.
39 H. Zhong, H. P. Xu and H. Zhang, *Chin. J. Anal. Chem.*, 2014, **42**, 475–481.
40 L. Shang, K. Nienhaus and G. U. Nienhaus, *J. Nanobiotechnol.*, 2014, **12**, 11.
41 L. Treuel, S. Brandholt, P. Maffre, S. Wiegele, L. Shang and G. U. Nienhaus, *ACS Nano*, 2014, **8**, 503–513.
42 L. Shang and S. J. Dong, *Anal. Chem.*, 2009, **81**, 1465–1470.
43 L. Shang, J. Y. Yin, J. Li, L. H. Jin and S. J. Dong, *Biosens. Bioelectron.*, 2009, **25**, 269–274.
44 S. Mura, G. Greppi, P. Innocenzi, M. Piccinini, C. Figus, M. L. Marongiu, C. L. Guo and J. Irudayaraj, *J. Raman Spectrosc.*, 2013, **44**, 35–40.
45 C. Wang, X. Q. Hao, M. Wang, C. L. Guo, B. Q. Xu, E. N. Tan, Y. Y. Zhang, Y. H. Yu, Z. Y. Li, H. B. Yang, M. P. Song and X. P. Li, *Chem. Sci.*, 2014, **5**, 1221–1226.
46 J. F. Zhou, S. Samanta, C. L. Guo, J. Locklin and B. Q. Xu, *Nanoscale*, 2013, **5**, 5715–5719.
47 Z. L. Liu, B. Zhao, C. L. Guo, Y. J. Sun, Y. Shi, H. B. Yang and Z. Li, *J. Colloid Interface Sci.*, 2010, **351**, 233–238.
48 F. G. Xu, C. L. Guo, Y. J. Sun, Z. L. Liu, Y. Zhang and Z. Li, *Colloids Surf., A*, 2010, **353**, 125–131.
49 L. L. Sun, Y. J. Sun, F. G. Xu, Y. Zhang, T. Yang, C. L. Guo, Z. L. Liu and Z. Li, *Nanotechnology*, 2009, **20**, 125502.
50 Z. L. Liu, B. Zhao, C. L. Guo, Y. J. Sun, F. G. Xu, H. B. Yang and Z. Li, *J. Phys. Chem. C*, 2009, **113**, 16766–16771.
51 L. Wang, G. Wei, C. L. Guo, L. L. Sun, Y. J. Sun, Y. G. Song, T. Yang and Z. Li, *Colloids Surf., A*, 2008, **312**, 148–153.
52 L. L. Sun, Y. H. Song, G. Wei, L. Wang, C. L. Guo, Y. J. Sun and Z. Li, *Chem. Lett.*, 2007, **36**, 142–143.
53 L. Wang, G. Wei, L. L. Sun, Z. G. Liu, Y. H. Song, T. Yang, Y. J. Sun, C. L. Guo and Z. Li, *Nanotechnology*, 2006, **17**, 2907–2912.
54 L. L. Sun, L. Wang, Y. H. Song, C. L. Guo, Y. J. Sun, C. Y. Peng, Z. L. Liu and Z. Li, *Appl. Surf. Sci.*, 2008, **254**, 2581–2587.
55 L. Wang, Y. H. Song, L. L. Sun, C. L. Guo, Y. J. Sun and Z. Li, *Mater. Lett.*, 2008, **62**, 4124–4126.
56 Y. H. Song, Z. Li, Z. G. Liu, G. Wei, L. Wang, L. L. Sun, C. L. Guo, Y. J. Sun and T. Yang, *J. Phys. Chem. B*, 2006, **110**, 10792–10798.
57 Y. Du, H. Wei, J. Z. Kang, J. L. Yan, X. B. Yin, X. R. Yang and E. K. Wang, *Anal. Chem.*, 2005, **77**, 7993–7997.
58 B. L. Li, Y. L. Wang, H. Wei and S. J. Dong, *Biosens. Bioelectron.*, 2008, **23**, 965–970.
59 L. Y. Fang, Z. Z. Lv, H. Wei and E. Wang, *Anal. Chim. Acta*, 2008, **628**, 80–86.
60 J. Li, Y. H. Xu, H. Wei, T. Huo and E. K. Wang, *Anal. Chem.*, 2007, **79**, 5439–5443.

61 J. Li, M. H. Huang, X. Q. Liu, H. Wei, Y. H. Xu, G. B. Xu and E. K. Wang, *Analyst*, 2007, **132**, 687–691.
62 J. G. Bai, H. Wei, B. L. Li, L. H. Song, L. Y. Fang, Z. Z. Lv, W. H. Zhou and E. K. Wang, *Chem.–Asian J.*, 2008, **3**, 1935–1941.
63 H. Wei, J. Y. Yin and E. Wang, *Anal. Chem.*, 2008, **80**, 5635–5639.
64 H. Wei, Y. Du, J. Z. Kang, G. B. Xu and E. K. Wang, *Chin. J. Chem.*, 2007, **25**, 159–163.
65 X. H. Gao, Y. Y. Cui, R. M. Levenson, L. W. K. Chung and S. M. Nie, *Nat. Biotechnol.*, 2004, **22**, 969–976.
66 M. Y. Han, X. H. Gao, J. Z. Su and S. Nie, *Nat. Biotechnol.*, 2001, **19**, 631–635.
67 X. M. Qian, X. H. Peng, D. O. Ansari, Q. Yin-Goen, G. Z. Chen, D. M. Shin, L. Yang, A. N. Young, M. D. Wang and S. M. Nie, *Nat. Biotechnol.*, 2008, **26**, 83–90.
68 J. Kong, N. R. Franklin, C. W. Zhou, M. G. Chapline, S. Peng, K. J. Cho and H. J. Dai, *Science*, 2000, **287**, 622–625.
69 Y. N. Xia, P. D. Yang, Y. G. Sun, Y. Y. Wu, B. Mayers, B. Gates, Y. D. Yin, F. Kim and Y. Q. Yan, *Adv. Mater.*, 2003, **15**, 353–389.
70 Y. Cui, Q. Q. Wei, H. K. Park and C. M. Lieber, *Science*, 2001, **293**, 1289–1292.
71 Y. Huang, X. F. Duan, Y. Cui, L. J. Lauhon, K. H. Kim and C. M. Lieber, *Science*, 2001, **294**, 1313–1317.
72 Z. N. Bao, J. A. Rogers and H. E. Katz, *J. Mater. Chem.*, 1999, **9**, 1895–1904.
73 S. H. Sun, C. B. Murray, D. Weller, L. Folks and A. Moser, *Science*, 2000, **287**, 1989–1992.
74 C. B. Murray, D. J. Norris and M. G. Bawendi, *J. Am. Chem. Soc.*, 1993, **115**, 8706–8715.
75 C. J. Murphy, T. K. San, A. M. Gole, C. J. Orendorff, J. X. Gao, L. Gou, S. E. Hunyadi and T. Li, *J. Phys. Chem. B*, 2005, **109**, 13857–13870.
76 P. K. Jain, X. H. Huang, I. H. El-Sayed and M. A. El-Sayed, *Acc. Chem. Res.*, 2008, **41**, 1578–1586.
77 A. M. Smith, H. W. Duan, A. M. Mohs and S. M. Nie, *Adv. Drug Delivery Rev.*, 2008, **60**, 1226–1240.
78 K. Saha, S. S. Agasti, C. Kim, X. N. Li and V. M. Rotello, *Chem. Rev.*, 2012, **112**, 2739–2779.
79 Z. Y. Tang, N. A. Kotov and M. Giersig, *Science*, 2002, **297**, 237–240.
80 Z. Y. Tang, Y. Wang, P. Podsiadlo and N. A. Kotov, *Adv. Mater.*, 2006, **18**, 3203–3224.
81 L. X. Zhang, P. C. Li, X. H. Liu, L. W. Du and E. Wang, *Adv. Mater.*, 2007, **19**, 4279–4283.
82 W. Yang, X. L. Wang, F. Yang, C. Yang and X. R. Yang, *Adv. Mater.*, 2008, **20**, 2579–2587.
83 Y. Jiang, H. Zhao, Y. Q. Lin, N. N. Zhu, Y. R. Ma and L. Q. Mao, *Angew. Chem., Int. Ed.*, 2010, **49**, 4800–4804.
84 Y. Jiang, H. Zhao, N. N. Zhu, Y. Q. Lin, P. Yu and L. Q. Mao, *Angew. Chem., Int. Ed.*, 2008, **47**, 8601–8604.
85 K. L. Ai, Y. L. Liu and L. H. Lu, *J. Am. Chem. Soc.*, 2009, **131**, 9496–9497.
86 L. L. Li, Q. Yin, J. J. Cheng and Y. Lu, *Adv. Healthcare Mater.*, 2012, **1**, 567–572.
87 L. L. Li, R. B. Zhang, L. L. Yin, K. Z. Zheng, W. P. Qin, P. R. Selvin and Y. Lu, *Angew. Chem., Int. Ed.*, 2012, **51**, 6121–6125.
88 L. L. Li, P. W. Wu, K. Hwang and Y. Lu, *J. Am. Chem. Soc.*, 2013, **135**, 2411–2414.
89 L. L. Li, M. Y. Xie, J. Wang, X. Y. Li, C. Wang, Q. Yuan, D. W. Pang, Y. Lu and W. H. Tan, *Chem. Commun.*, 2013, **49**, 5823–5825.
90 Y. D. Jin, D. Cahen, N. Friedman and M. Sheves, *Angew. Chem., Int. Ed.*, 2006, **45**, 6325–6328.
91 E. M. Saurer, R. M. Flessner, S. P. Sullivan, M. R. Prausnitz and D. M. Lynn, *Biomacromolecules*, 2010, **11**, 3136–3143.
92 S. K. M. Nalluri, C. Berdugo, N. Javid, P. Frederix and R. V. Ulijn, *Angew. Chem., Int. Ed.*, 2014, **53**, 5882–5887.
93 L. Kabalah-Amitai, B. Mayzel, Y. Kauffmann, A. N. Fitch, L. Bloch, P. Gilbert and B. Pokroy, *Science*, 2013, **340**, 454–457.
94 M. Reches and E. Gazit, *Science*, 2003, **300**, 625–627.
95 H. Wei, B. L. Li, Y. Du, S. J. Dong and E. Wang, *Chem. Mater.*, 2007, **19**, 2987–2993.
96 H. Wei and E. K. Wang, *Nanotechnology*, 2007, **18**, 295603.
97 H. Wei, J. Li, Y. L. Wang and E. K. Wang, *Nanotechnology*, 2007, **18**, 175610.
98 C. L. Guo, Y. H. Song, L. Wang, L. L. Sun, Y. J. Sun, C. Y. Peng, Z. L. Liu, T. Yang and Z. Li, *J. Phys. Chem. B*, 2008, **112**, 1022–1027.
99 C. L. Guo, G. P. Li, Z. L. Liu, L. L. Sun, Y. J. Sun, F. G. Xu, Y. Zhang, T. Yang and Z. Li, *ChemPhysChem*, 2009, **10**, 1624–1629.
100 C. L. Guo, Z. L. Liu, F. G. Xu, L. L. Sun, Y. J. Sun, T. Yang and Z. Li, *J. Phys. Chem. B*, 2009, **113**, 6068–6073.
101 Z. D. Wang, J. Q. Zhang, J. M. Ekman, P. J. A. Kenis and Y. Lu, *Nano Lett.*, 2010, **10**, 1886–1891.
102 C. Y. Chiu, Y. J. Li, L. Y. Ruan, X. C. Ye, C. B. Murray and Y. Huang, *Nat. Chem.*, 2011, **3**, 393–399.
103 G. Tikhomirov, S. Hoogland, P. E. Lee, A. Fischer, E. H. Sargent and S. O. Kelley, *Nat. Nanotechnol.*, 2011, **6**, 485–490.
104 Z. Zhao, E. L. Jacovetty, Y. Liu and H. Yan, *Angew. Chem., Int. Ed.*, 2011, **50**, 2041–2044.
105 D. K. Lim, K. S. Jeon, J. H. Hwang, H. Kim, S. Kwon, Y. D. Suh and J. M. Nam, *Nat. Nanotechnol.*, 2011, **6**, 452–460.
106 Z. D. Wang, L. H. Tang, L. H. Tan, J. H. Li and Y. Lu, *Angew. Chem., Int. Ed.*, 2012, **51**, 9078–9082.
107 L. Y. T. Chou, K. Zagorovsky and W. C. W. Chan, *Nat. Nanotechnol.*, 2014, **9**, 148–155.
108 A. L. Margolin and M. A. Navia, *Angew. Chem., Int. Ed.*, 2001, **40**, 2204–2222.
109 M. L. Flenniken, D. A. Willits, S. Brumfield, M. J. Young and T. Douglas, *Nano Lett.*, 2003, **3**, 1573–1576.
110 J. C. Falkner, M. E. Turner, J. K. Bosworth, T. J. Trentler, J. E. Johnson, T. W. Lin and V. L. Colvin, *J. Am. Chem. Soc.*, 2005, **127**, 5274–5275.
111 C. A. Butts, J. Swift, S. G. Kang, L. Di Costanzo, D. W. Christianson, J. G. Saven and I. J. Dmochowski, *Biochemistry*, 2008, **47**, 12729–12739.

112 M. Suzuki, M. Abe, T. Ueno, S. Abe, T. Goto, Y. Toda, T. Akita, Y. Yamadae and Y. Watanabe, *Chem. Commun.*, 2009, 4871–4873.
113 P. L. Xavier, K. Chaudhari, P. K. Verma, S. K. Pal and T. Pradeep, *Nanoscale*, 2010, **2**, 2769–2776.
114 M. Guli, E. M. Lambert, M. Li and S. Mann, *Angew. Chem., Int. Ed.*, 2010, **49**, 520–523.
115 A. Mathew, P. R. Sajanlal and T. Pradeep, *J. Mater. Chem.*, 2011, **21**, 11205–11212.
116 H. W. Li, K. L. Ai and Y. Q. Wu, *Chem. Commun.*, 2011, **47**, 9852–9854.
117 C. L. Guo and J. Irudayaraj, *Anal. Chem.*, 2011, **83**, 2883–2889.
118 C. Guo, B. Book-Newell and J. Irudayaraj, *Chem. Commun.*, 2011, **47**, 12658–12660.
119 D. C. Bassett, L. M. Grover, F. A. Muller, M. D. McKee and J. E. Barralet, *Adv. Funct. Mater.*, 2011, **21**, 2968–2977.
120 K. Chaudhari, P. L. Xavier and T. Pradeep, *ACS Nano*, 2011, **5**, 8816–8827.
121 T. H. Chen and W. L. Tseng, *Small*, 2012, **8**, 1912–1919.
122 H. Y. Li, H. L. Xin, D. A. Muller and L. A. Estroff, *Science*, 2009, **326**, 1244–1247.
123 V. Berry, A. Gole, S. Kundu, C. J. Murphy and R. F. Saraf, *J. Am. Chem. Soc.*, 2005, **127**, 17600–17601.
124 T. J. Park, S. Y. Lee, N. S. Heo and T. S. Seo, *Angew. Chem., Int. Ed.*, 2010, **49**, 7019–7024.
125 K. T. Nam, D. W. Kim, P. J. Yoo, C. Y. Chiang, N. Meethong, P. T. Hammond, Y. M. Chiang and A. M. Belcher, *Science*, 2006, **312**, 885–888.
126 Y. J. Lee, H. Yi, W. J. Kim, K. Kang, D. S. Yun, M. S. Strano, G. Ceder and A. M. Belcher, *Science*, 2009, **324**, 1051–1055.
127 H. F. Bao, Z. S. Lu, X. Q. Cui, Y. Qiao, J. Guo, J. M. Anderson and C. M. Li, *Acta Biomater.*, 2010, **6**, 3534–3541.
128 S. R. Sturzenbaum, M. Hockner, A. Panneerselvam, J. Levitt, J. S. Bouillard, S. Taniguchi, L. A. Dailey, R. A. Khanbeigi, E. V. Rosca, M. Thanou, K. Suhling, A. V. Zayats and M. Green, *Nat. Nanotechnol.*, 2013, **8**, 57–60.
129 J. L. Wang, G. Zhang, Q. W. Li, H. Jiang, C. Y. Liu, C. Amatore and X. M. Wang, *Sci. Rep.*, 2013, **3**, 1157.
130 S. P. Gao, D. H. Chen, Q. W. Li, J. Ye, H. Jiang, C. Amatore and X. M. Wang, *Sci. Rep.*, 2014, **4**, 4384.
131 G. L. Liu, Q. Feng, X. Y. Mu, W. J. Zheng, T. F. Chen, L. Qi and D. Li, *J. Mater. Chem. B*, 2013, **1**, 2128–2131.
132 G. Q. Wang, H. Mitomo, Y. Matsuo, N. Shimamoto, K. Niikura and K. Ijiro, *J. Mater. Chem. B*, 2013, **1**, 5899–5907.
133 M. Wysokowski, M. Motylenko, H. Stocker, V. V. Bazhenov, E. Langer, A. Dobrowolska, K. Czaczyk, R. Galli, A. L. Stelling, T. Behm, L. Klapiszewski, D. Ambrozewicz, M. Nowacka, S. L. Molodtsov, B. Abendroth, D. C. Meyer, K. J. Kurzydlowski, T. Jesionowski and H. Ehrlich, *J. Mater. Chem. B*, 2013, **1**, 6469–6476.
134 Z. Zhen, W. Tang, C. Guo, H. Chen, X. Lin, G. Liu, B. Fei, X. Chen, B. Xu and J. Xie, *ACS Nano*, 2013, **7**, 6988–6996.
135 Z. X. Zhou, W. Wei, Y. J. Zhang and S. Q. Liu, *J. Mater. Chem. B*, 2013, **1**, 2851–2858.
136 B. Soptei, L. N. Nagy, P. Baranyai, I. Szabo, G. Mezo, F. Hudecz and A. Bota, *Gold Bull.*, 2013, **46**, 195–203.
137 X. H. Liu, L. X. Zhang, Y. L. Wang, C. L. Guo and E. K. Wang, *Cryst. Growth Des.*, 2008, **8**, 759–762.
138 Y. J. Sun, L. L. Sun, F. G. Xu, C. L. Guo, Z. L. Liu, Y. Zhang, T. Yang and Z. Li, *Appl. Surf. Sci.*, 2009, **255**, 6814–6818.
139 Y. J. Sun, L. L. Sun, B. H. Zhang, F. G. Xu, Z. L. Liu, C. L. Guo, Y. Zhang and Z. Li, *Talanta*, 2009, **79**, 562–569.
140 L. L. Sun, Y. H. Song, L. Wang, Y. J. Sun, C. L. Guo, Z. L. Liu and Z. Li, *J. Nanosci. Nanotechnol.*, 2008, **8**, 4415–4423.
141 Y. J. Sun, G. Wei, Y. H. Song, L. Wang, L. L. Sun, C. L. Guo, T. Yang and Z. Li, *Nanotechnology*, 2008, **19**, 115604.
142 Y. H. Song, C. L. Guo, L. L. Sun, G. Wei, C. Y. Peng, L. Wang, Y. J. Sun and Z. Li, *J. Phys. Chem. B*, 2007, **111**, 461–468.
143 Y. J. Sun, L. Wang, L. L. Sun, C. L. Guo, T. Yang, Z. L. Liu, F. G. Xu and Z. Li, *J. Chem. Phys.*, 2008, **128**, 074704.
144 W. Shenton, T. Douglas, M. Young, G. Stubbs and S. Mann, *Adv. Mater.*, 1999, **11**, 253–256.
145 T. Ueno, M. Suzuki, T. Goto, T. Matsumoto, K. Nagayama and Y. Watanabe, *Angew. Chem., Int. Ed.*, 2004, **43**, 2527–2530.
146 N. Goswami, A. Giri, S. Kar, M. S. Bootharaju, R. John, P. L. Xavier, T. Pradeep and S. K. Pal, *Small*, 2012, **8**, 3175–3184.
147 M. Reches and E. Gazit, *Nat. Nanotechnol.*, 2006, **1**, 195–200.
148 L. Fabris, S. Antonello, L. Armelao, R. L. Donkers, F. Polo, C. Toniolo and F. Maran, *J. Am. Chem. Soc.*, 2006, **128**, 326–336.
149 I. Ron, I. Pecht, M. Sheves and D. Cahen, *Acc. Chem. Res.*, 2010, **43**, 945–953.
150 A. Gitelman and H. Rapaport, *Langmuir*, 2014, **30**, 4716–4724.
151 A. Brif, G. Ankonina, C. Drathen and B. Pokroy, *Adv. Mater.*, 2014, **26**, 477–481.
152 G. Pieters, C. Pezzato and L. J. Prins, *J. Am. Chem. Soc.*, 2012, **134**, 15289–15292.
153 M. Ritenberg, E. Beilis, A. Ilovitsh, Z. Barkai, A. Shahmoon, S. Richter, Z. Zalevsky and R. Jelinek, *Sci. Rep.*, 2014, **4**, 3666.
154 J. P. Xie, Y. G. Zheng and J. Y. Ying, *J. Am. Chem. Soc.*, 2009, **131**, 888–889.
155 H. Wei, Z. D. Wang, L. M. Yang, S. L. Tian, C. J. Hou and Y. Lu, *Analyst*, 2010, **135**, 1406–1410.
156 J. P. Xie, Y. G. Zheng and J. Y. Ying, *Chem. Commun.*, 2010, **46**, 961–963.
157 C. L. Liu, H. T. Wu, Y. H. Hsiao, C. W. Lai, C. W. Shih, Y. K. Peng, K. C. Tang, H. W. Chang, Y. C. Chien, J. K. Hsiao, J. T. Cheng and P. T. Chou, *Angew. Chem., Int. Ed.*, 2011, **50**, 7056–7060.
158 M. Colombo, S. Mazzucchelli, V. Collico, S. Avvakumova, L. Pandolfi, F. Corsi, F. Porta and D. Prosperi, *Angew. Chem., Int. Ed.*, 2012, **51**, 9272–9275.
159 H. Wei, Z. D. Wang, J. O. Zhang, S. House, Y. G. Gao, L. M. Yang, H. Robinson, L. H. Tan, H. Xing, C. J. Hou, I. M. Robertson, J. M. Zuo and Y. Lu, *Nat. Nanotechnol.*, 2011, **6**, 93–97.

160 Z. Xu, X. W. Liu, Y. S. Ma and H. W. Gao, *Environ. Sci. Pollut. Res.*, 2010, **17**, 798–806.
161 H. R. Luckarift, M. B. Dickerson, K. H. Sandhage and J. C. Spain, *Small*, 2006, **2**, 640–643.
162 H. Wei, S. House, J. J. X. Wu, J. Zhang, Z. D. Wang, Y. He, E. J. Gao, Y. G. Gao, H. Robinson, W. Li, J. M. Zuo, I. M. Robertson and Y. Lu, *Nano Res.*, 2013, **6**, 627–634.
163 L. Ma, H. Y. Liu, Z. C. Zhu, H. L. Wang, X. Y. Xu, N. Na and O. Y. Jin, *J. Mater. Chem. A*, 2013, **1**, 15082–15088.
164 M. W. England, E. M. Lambert, M. Li, L. Turyanska, A. J. Patil and S. Mann, *Nanoscale*, 2012, **4**, 6710–6713.
165 T. Shiomi, T. Tsunoda, A. Kawai, F. Mizukami and K. Sakaguchi, *Chem. Mater.*, 2007, **19**, 4486–4493.
166 B. H. San, S. Lee, S. H. Moh, J. G. Park, J. H. Lee, H. Y. Hwang and K. K. Kim, *J. Mater. Chem. B*, 2013, **1**, 1453–1460.
167 R. E. Canfield, *J. Biol. Chem.*, 1963, **238**, 2698–2707.
168 M. J. Panzner, S. M. Bilinovich, W. J. Youngs and T. C. Leeper, *Chem. Commun.*, 2011, **47**, 12479–12481.
169 S. Abe, M. Tsujimoto, K. Yoneda, M. Ohba, T. Hikage, M. Takano, S. Kitagawa and T. Ueno, *Small*, 2012, **8**, 1314–1319.
170 C. Liu, D. Yang, Y. Jiao, Y. Tian, Y. G. Wang and Z. Y. Jiang, *ACS Appl. Mater. Interfaces*, 2013, **5**, 3824–3832.
171 T. Yang, Z. Li, L. Wang, C. L. Guo and Y. J. Sun, *Langmuir*, 2007, **23**, 10533–10538.
172 T. Y. Zhou, Y. H. Huang, W. B. Li, Z. M. Cai, F. Luo, C. J. Yang and X. Chen, *Nanoscale*, 2012, **4**, 5312–5315.
173 M. Sarikaya, C. Tamerler, A. K. Y. Jen, K. Schulten and F. Baneyx, *Nat. Mater.*, 2003, **2**, 577–585.
174 M. Uchida, M. T. Klem, M. Allen, P. Suci, M. Flenniken, E. Gillitzer, Z. Varpness, L. O. Liepold, M. Young and T. Douglas, *Adv. Mater.*, 2007, **19**, 1025–1042.
175 M. B. Dickerson, K. H. Sandhage and R. R. Naik, *Chem. Rev.*, 2008, **108**, 4935–4978.
176 R. V. Ulijn and A. M. Smith, *Chem. Soc. Rev.*, 2008, **37**, 664–675.
177 L. Berti and G. A. Burley, *Nat. Nanotechnol.*, 2008, **3**, 81–87.
178 Z. D. Wang and Y. Lu, *J. Mater. Chem.*, 2009, **19**, 1788–1798.
179 R. de la Rica and H. Matsui, *Chem. Soc. Rev.*, 2010, **39**, 3499–3509.
180 J. M. Slocik and R. R. Naik, *Chem. Soc. Rev.*, 2010, **39**, 3454–3463.
181 C. L. Chen and N. L. Rosi, *Angew. Chem., Int. Ed.*, 2010, **49**, 1924–1942.
182 M. R. Jones, K. D. Osberg, R. J. Macfarlane, M. R. Langille and C. A. Mirkin, *Chem. Rev.*, 2011, **111**, 3736–3827.
183 J. M. Galloway and S. S. Staniland, *J. Mater. Chem.*, 2012, **22**, 12423–12434.
184 D. M. Chevrier, A. Chatt and P. Zhang, *J. Nanophotonics*, 2012, **6**, 064504.
185 V. Bonacic-Koutecky, A. Kulesza, L. Gell, R. Mitric, R. Antoine, F. Bertorelle, R. Hamouda, D. Rayane, M. Broyer, T. Tabarin and P. Dugourd, *Phys. Chem. Chem. Phys.*, 2012, **14**, 9282–9290.
186 S. T. Yang, Y. Liu, Y. W. Wang and A. N. Cao, *Small*, 2013, **9**, 1635–1653.
187 C. Y. Chiu, L. Y. Ruan and Y. Huang, *Chem. Soc. Rev.*, 2013, **42**, 2512–2527.
188 K. E. Sapsford, W. R. Algar, L. Berti, K. B. Gemmill, B. J. Casey, E. Oh, M. H. Stewart and I. L. Medintz, *Chem. Rev.*, 2013, **113**, 1904–2074.
189 N. J. M. Sanghamitra and T. Ueno, *Chem. Commun.*, 2013, **49**, 4114–4126.
190 T. Ueno, *Chem.–Eur. J.*, 2013, **19**, 9096–9102.
191 E. Gazit, *Chem. Soc. Rev.*, 2007, **36**, 1263–1269.
192 T. P. J. Knowles, T. W. Oppenheim, A. K. Buell, D. Y. Chirgadze and M. E. Welland, *Nat. Nanotechnol.*, 2010, **5**, 204–207.
193 J. B. Xie, M. Qin, Y. Cao and W. Wang, *Proteins*, 2011, **79**, 2505–2516.
194 J. B. Xie, Y. Cao, H. Pan, M. Qin, Z. Q. Yan, X. Xiong and W. Wang, *Proteins*, 2012, **80**, 2501–2513.
195 F. Cavalieri, M. Ashokkumar, F. Grieser and F. Caruso, *Langmuir*, 2008, **24**, 10078–10083.
196 M. F. Zhou, T. S. H. Leong, S. Melino, F. Cavalieri, S. Kentish and M. Ashokkumar, *Ultrason. Sonochem.*, 2010, **17**, 333–337.
197 Q.-Q. Gai, F. Qu, Z.-J. Liu, R.-J. Dai and Y.-K. Zhang, *J. Chromatogr. A*, 2010, **1217**, 5035–5042.
198 G. Fu, H. He, Z. Chai, H. Chen, J. Kong, Y. Wang and Y. Jiang, *Anal. Chem.*, 2011, **83**, 1431–1436.
199 Z. Lin, Z. Xia, J. Zheng, D. Zheng, L. Zhang, H. Yang and G. Chen, *J. Mater. Chem.*, 2012, **22**, 17914–17922.
200 G. Pan, Q. Guo, C. Cao, H. Yang and B. Li, *Soft Matter*, 2013, **9**, 3840–3850.
201 Z. Lin, Y. Lin, X. Sun, H. Yang, L. Zhang and G. Chen, *J. Chromatogr. A*, 2013, **1284**, 8–16.
202 X. Li, B. Zhang, L. Tian, W. Li, T. Xin, H. Zhang and Q. Zhang, *Sens. Actuators, B*, 2014, **196**, 265–271.
203 J. Cao, X. Zhang, X. He, L. Chen and Y. Zhang, *Chem.–Asian J.*, 2014, **9**, 526–533.
204 H. Chen, J. Kong, D. Yuan and G. Fu, *Biosens. Bioelectron.*, 2014, **53**, 5–11.
205 L. A. Peyser, A. E. Vinson, A. P. Bartko and R. M. Dickson, *Science*, 2001, **291**, 103–106.
206 J. T. Petty, J. Zheng, N. V. Hud and R. M. Dickson, *J. Am. Chem. Soc.*, 2004, **126**, 5207–5212.
207 P. D. Jadzinsky, G. Calero, C. J. Ackerson, D. A. Bushnell and R. D. Kornberg, *Science*, 2007, **318**, 430–433.
208 W. W. Guo, J. P. Yuan, Q. Z. Dong and E. K. Wang, *J. Am. Chem. Soc.*, 2010, **132**, 932–934.
209 L. Shang, S. J. Dong and G. U. Nienhaus, *Nano Today*, 2011, **6**, 401–418.
210 S. Choi, R. M. Dickson and J. H. Yu, *Chem. Soc. Rev.*, 2012, **41**, 1867–1891.
211 Y. Z. Lu and W. Chen, *Chem. Soc. Rev.*, 2012, **41**, 3594–3623.
212 Y. C. Shiang, C. C. Huang, W. Y. Chen, P. C. Chen and H. T. Chang, *J. Mater. Chem.*, 2012, **22**, 12972–12982.
213 J. Zheng, C. Zhou, M. X. Yu and J. B. Liu, *Nanoscale*, 2012, **4**, 4073–4083.

214 X. Yuan, Z. T. Luo, Y. Yu, Q. F. Yao and J. P. Xie, *Chem.–Asian J.*, 2013, **8**, 858–871.
215 H. Kawasaki, K. Hamaguchi, I. Osaka and R. Arakawa, *Adv. Funct. Mater.*, 2011, **21**, 3508–3515.
216 L. Shang, F. Stockmar, N. Azadfar and G. U. Nienhaus, *Angew. Chem., Int. Ed.*, 2013, **52**, 11154–11157.
217 L. B. Zhang, J. B. Zhu, S. J. Guo, T. Li, J. Li and E. K. Wang, *J. Am. Chem. Soc.*, 2013, **135**, 2403–2406.
218 L. B. Zhang and E. K. Wang, *Nano Today*, 2014, **9**, 132–157.
219 J. F. Parker, C. A. Fields-Zinna and R. W. Murray, *Acc. Chem. Res.*, 2010, **43**, 1289–1296.
220 A. Desireddy, B. E. Conn, J. Guo, B. Yoon, R. N. Barnett, B. M. Monahan, K. Kirschbaum, W. P. Griffith, R. L. Whetten, U. Landman and T. P. Bigioni, *Nature*, 2013, **501**, 399–402.
221 H. Yang, Y. Wang, H. Huang, L. Gell, L. Lehtovaara, S. Malola, H. Häkkinen and N. Zheng, *Nat. Commun.*, 2013, **4**, 2422.
222 S. Antonello, G. Arrigoni, T. Dainese, M. De Nardi, G. Parisio, L. Perotti, A. Rene, A. Venzo and F. Maran, *ACS Nano*, 2014, **8**, 2788–2795.
223 T. Dainese, S. Antonello, J. A. Gascon, F. F. Pan, N. V. Perera, M. Ruzzi, A. Venzo, A. Zoleo, K. Rissanen and F. Maran, *ACS Nano*, 2014, **8**, 3904–3912.
224 L. Shang and S. Dong, *Chem. Commun.*, 2008, 1088–1090.
225 L. Shang and S. J. Dong, *J. Mater. Chem.*, 2008, **18**, 4636–4640.
226 L. Shang, R. M. Dorlich, S. Brandholt, R. Schneider, V. Trouillet, M. Bruns, D. Gerthsen and G. U. Nienhaus, *Nanoscale*, 2011, **3**, 2009–2014.
227 L. Shang, N. Azadfar, F. Stockmar, W. Send, V. Trouillet, M. Bruns, D. Gerthsen and G. U. Nienhaus, *Small*, 2011, **7**, 2614–2620.
228 L. Shang, S. Brandholt, F. Stockmar, V. Trouillet, M. Bruns and G. U. Nienhaus, *Small*, 2012, **8**, 661–665.
229 L. Shang and G. U. Nienhaus, *Biophys. Rev.*, 2012, **4**, 313–322.
230 L. Shang and G. U. Nienhaus, *Mater. Today*, 2013, **16**, 58–66.
231 R. Jin, *Nanoscale*, 2010, **2**, 343–362.
232 G. Li, C. Zeng and R. Jin, *J. Am. Chem. Soc.*, 2014, **136**, 3673–3679.
233 Z. Luo, K. Zheng and J. Xie, *Chem. Commun.*, 2014, **50**, 5143–5155.
234 Y. Yu, Z. T. Luo, C. S. Teo, Y. N. Tan and J. P. Xie, *Chem. Commun.*, 2013, **49**, 9740–9742.
235 X.-D. Zhang, Z. Luo, J. Chen, X. Shen, S. Song, Y. Sun, S. Fan, F. Fan, D. T. Leong and J. Xie, *Adv. Mater.*, 2014, **26**, 4565–4568.
236 W. Wei, Y. Lu, W. Chen and S. Chen, *J. Am. Chem. Soc.*, 2011, **133**, 2060–2063.
237 M. Liu and W. Chen, *Nanoscale*, 2013, **5**, 12558–12564.
238 J. Sun, J. Zhang and Y. Jin, *J. Mater. Chem. C*, 2013, **1**, 138–143.
239 R. L. Whetten, M. N. Shafigullin, J. T. Khoury, T. G. Schaaff, I. Vezmar, M. M. Alvarez and A. Wilkinson, *Acc. Chem. Res.*, 1999, **32**, 397–406.
240 M. Walter, J. Akola, O. Lopez-Acevedo, P. D. Jadzinsky, G. Calero, C. J. Ackerson, R. L. Whetten, H. Grönbeck and H. Häkkinen, *Proc. Natl. Acad. Sci. U. S. A.*, 2008, **105**, 9157–9162.
241 Z. H. Qing, X. X. He, T. P. Qing, K. M. Wang, H. Shi, D. G. He, Z. Zou, L. Yan, F. Z. Xu, X. S. Ye and Z. G. Mao, *Anal. Chem.*, 2013, **85**, 12138–12143.
242 L. H. Jin, Y. X. Fang, L. Shang, Y. Q. Liu, J. Li, L. Wang, P. Hu and S. J. Dong, *Chem. Commun.*, 2013, **49**, 243–245.
243 L. Shang, L. X. Yang, F. Stockmar, R. Popescu, V. Trouillet, M. Bruns, D. Gerthsen and G. U. Nienhaus, *Nanoscale*, 2012, **4**, 4155–4160.
244 L. H. Jin, L. Shang, S. J. Guo, Y. X. Fang, D. Wen, L. Wang, J. Y. Yin and S. J. Dong, *Biosens. Bioelectron.*, 2011, **26**, 1965–1969.
245 L. Shang and S. J. Dong, *Biosens. Bioelectron.*, 2009, **24**, 1569–1573.
246 X. Yuan, B. Zhang, Z. T. Luo, Q. F. Yao, D. T. Leong, N. Yan and J. P. Xie, *Angew. Chem., Int. Ed.*, 2014, **53**, 4623–4627.
247 Q. F. Yao, Z. T. Luo, X. Yuan, Y. Yu, C. Zhang, J. P. Xie and J. Y. Lee, *Sci. Rep.*, 2014, **4**, 3848.
248 X. D. Zhang, J. Chen, Z. T. Luo, D. Wu, X. Shen, S. S. Song, Y. M. Sun, P. X. Liu, J. Zhao, S. D. Huo, S. J. Fan, F. Y. Fan, X. J. Liang and J. P. Xie, *Adv. Healthcare Mater.*, 2014, **3**, 133–141.
249 X. Yuan, M. I. Setyawati, A. S. Tan, C. N. Ong, D. T. Leong and J. P. Xie, *NPG Asia Mater.*, 2013, **5**, e39.
250 D. Y. Chen, Z. T. Luo, N. J. Li, J. Y. Lee, J. P. Xie and J. M. Lu, *Adv. Funct. Mater.*, 2013, **23**, 4324–4331.
251 Y. Yu, Q. F. Yao, Z. T. Luo, X. Yuan, J. Y. Lee and J. P. Xie, *Nanoscale*, 2013, **5**, 4606–4620.
252 X. Yuan, Y. Q. Tay, X. Y. Dou, Z. T. Luo, D. T. Leong and J. P. Xie, *Anal. Chem.*, 2013, **85**, 1913–1919.
253 C. J. Liu, J. Ling, X. Q. Zhang, J. Peng, Q. E. Cao and Z. T. Ding, *Anal. Methods*, 2013, **5**, 5584–5588.
254 A. Som, A. K. Samal, T. Udayabhaskararao, M. S. Bootharaju and T. Pradeep, *Chem. Mater.*, 2014, **26**, 3049–3056.
255 J. Hassinen, P. Pulkkinen, E. Kalenius, T. Pradeep, H. Tenhu, H. Hakkinen and R. H. A. Ras, *J. Phys. Chem. Lett.*, 2014, **5**, 585–589.
256 K. R. Krishnadas, T. Udayabhaskararao, S. Choudhury, N. Goswami, S. K. Pal and T. Pradeep, *Eur. J. Inorg. Chem.*, 2014, **2014**, 908–916.
257 A. Mathew, G. Natarajan, L. Lehtovaara, H. Hakkinen, R. M. Kumar, V. Subramanian, A. Jaleel and T. Pradeep, *ACS Nano*, 2014, **8**, 139–152.
258 I. Chakraborty, W. Kurashige, K. Kanehira, L. Gell, H. Hakkinen, Y. Negishi and T. Pradeep, *J. Phys. Chem. Lett.*, 2013, **4**, 3351–3355.
259 I. Chakraborty, S. Bag, U. Landman and T. Pradeep, *J. Phys. Chem. Lett.*, 2013, **4**, 2769–2773.
260 M. S. Bootharaju and T. Pradeep, *Langmuir*, 2013, **29**, 8125–8132.
261 S. Kumar, E. S. Shibu, T. Pradeep and A. K. Sood, *Opt. Express*, 2013, **21**, 8483–8492.

262 Y. Niihori, M. Matsuzaki, T. Pradeep and Y. Negishi, *J. Am. Chem. Soc.*, 2013, **135**, 4946–4949.
263 A. Ganguly, I. Chakraborty, T. Udayabhaskararao and T. Pradeep, *J. Nanopart. Res.*, 2013, **15**, 7.
264 K. S. Sugi, I. Chakraborty, T. Udayabhaskararao, J. S. Mohanty and T. Pradeep, *Part. Part. Syst. Charact.*, 2013, **30**, 241–243.
265 T. Udayabhaskararao, M. S. Bootharaju and T. Pradeep, *Nanoscale*, 2013, **5**, 9404–9411.
266 I. Chakraborty, T. Udayabhaskararao, G. K. Deepesh and T. Pradeep, *J. Mater. Chem. B*, 2013, **1**, 4059–4064.
267 M. S. Bootharaju, G. K. Deepesh, T. Udayabhaskararao and T. Pradeep, *J. Mater. Chem. A*, 2013, **1**, 611–620.
268 K. P. Remya, T. Udayabhaskararao and T. Pradeep, *J. Phys. Chem. C*, 2012, **116**, 26019–26026.
269 I. Chakraborty, A. Govindarajan, J. Erusappan, A. Ghosh, T. Pradeep, B. Yoon, R. L. Whetten and U. Landman, *Nano Lett.*, 2012, **12**, 5861–5866.
270 I. Chakraborty, T. Udayabhaskararao and T. Pradeep, *J. Hazard. Mater.*, 2012, **211**, 396–403.
271 A. George, E. S. Shibu, S. M. Maliyekkal, M. S. Bootharaju and T. Pradeep, *ACS Appl. Mater. Interfaces*, 2012, **4**, 639–644.
272 T. Udayabhaskararao, Y. Sun, N. Goswami, S. K. Pal, K. Balasubramanian and T. Pradeep, *Angew. Chem., Int. Ed.*, 2012, **51**, 2155–2159.
273 M. S. Bootharaju and T. Pradeep, *Langmuir*, 2011, **27**, 8134–8143.
274 E. S. Shibu and T. Pradeep, *Chem. Mater.*, 2011, **23**, 989–999.
275 M. A. H. Muhammed and T. Pradeep, *Small*, 2011, **7**, 204–208.
276 T. U. B. Rao, B. Nataraju and T. Pradeep, *J. Am. Chem. Soc.*, 2010, **132**, 16304–16307.
277 W. W. Guo, R. Orbach, I. Mironi-Harpaz, D. Seliktar and I. Willner, *Small*, 2013, **9**, 3748–3752.
278 R. Orbach, W. W. Guo, F. Wang, O. Lioubashevski and I. Willner, *Langmuir*, 2013, **29**, 13066–13071.
279 X. Q. Liu, F. Wang, A. Niazov-Elkan, W. W. Guo and I. Willner, *Nano Lett.*, 2013, **13**, 309–314.
280 J. Ai, W. W. Guo, B. L. Li, T. Li, D. Li and E. K. Wang, *Talanta*, 2012, **88**, 450–455.
281 W. W. Guo, J. P. Yuan and E. K. Wang, *Chem. Commun.*, 2012, **48**, 3076–3078.
282 J. P. Yuan, W. W. Guo and E. K. Wang, *Anal. Chim. Acta*, 2011, **706**, 338–342.
283 W. W. Guo, J. P. Yuan and E. K. Wang, *Chem. Commun.*, 2011, **47**, 10930–10932.
284 X. Yang, X. P. Sun, Z. Z. Lv, W. W. Guo, Y. Du and E. K. Wang, *Chem. Commun.*, 2010, **46**, 8818–8820.
285 W. W. Guo, J. P. Yuan and E. K. Wang, *Chem. Commun.*, 2009, 3395–3397.
286 S. Antonello, A. H. Holm, E. Instuli and F. Maran, *J. Am. Chem. Soc.*, 2007, **129**, 9836–9837.
287 S. Antonello, M. Hesari, F. Polo and F. Maran, *Nanoscale*, 2012, **4**, 5333–5342.
288 S. Antonello, N. V. Perera, M. Ruzzi, J. A. Gascon and F. Maran, *J. Am. Chem. Soc.*, 2013, **135**, 15585–15594.
289 S. Das, A. Goswami, M. Hesari, J. F. Al-Sharab, E. Mikmekova, F. Maran and T. Asefa, *Small*, 2014, **10**, 1473–1478.
290 M. A. H. Muhammed, P. K. Verma, S. K. Pal, A. Retnakumari, M. Koyakutty, S. Nair and T. Pradeep, *Chem.–Eur. J.*, 2010, **16**, 10103–10112.
291 X. Le Guevel, B. Hotzer, G. Jung, K. Hollemeyer, V. Trouillet and M. Schneider, *J. Phys. Chem. C*, 2011, **115**, 10955–10963.
292 F. Wen, Y. H. Dong, L. Feng, S. Wang, S. C. Zhang and X. R. Zhang, *Anal. Chem.*, 2011, **83**, 1193–1196.
293 Y. C. Wang, Y. Wang, F. B. Zhou, P. Kim and Y. N. Xia, *Small*, 2012, **8**, 3769–3773.
294 J. S. Mohanty, P. L. Xavier, K. Chaudhari, M. S. Bootharaju, N. Goswami, S. K. Pal and T. Pradeep, *Nanoscale*, 2012, **4**, 4255–4262.
295 S. K. Sun, L. X. Dong, Y. Cao, H. R. Sun and X. P. Yan, *Anal. Chem.*, 2013, **85**, 8436–8441.
296 H. W. Li, Y. Yue, T. Y. Liu, D. M. Li and Y. Q. Wu, *J. Phys. Chem. C*, 2013, **117**, 16159–16165.
297 J. M. Liu, J. T. Chen and X. P. Yan, *Anal. Chem.*, 2013, **85**, 3238–3245.
298 S. Ghosh, U. Anand and S. Mukherjee, *Anal. Chem.*, 2014, **86**, 3188–3194.
299 R. Ghosh, A. K. Sahoo, S. S. Ghosh, A. Paul and A. Chattopadhyay, *ACS Appl. Mater. Interfaces*, 2014, **6**, 3822–3828.
300 N. Goswami, A. Baksi, A. Giri, P. L. Xavier, G. Basu, T. Pradeep and S. K. Pal, *Nanoscale*, 2014, **6**, 1848–1854.
301 Y. L. Liu, K. L. Ai, X. L. Cheng, L. H. Huo and L. H. Lu, *Adv. Funct. Mater.*, 2010, **20**, 951–956.
302 N. Goswami, A. Giri, M. S. Bootharaju, P. L. Xavier, T. Pradeep and S. K. Pal, *Anal. Chem.*, 2011, **83**, 9676–9680.
303 K. Choudhari, P. L. Xavier and T. Pradeep, *J. Biomed. Nanotechnol.*, 2011, **7**, 70–71.
304 A. H. Holm, M. Ceccato, R. L. Donkers, L. Fabris, G. Pace and F. Maran, *Langmuir*, 2006, **22**, 10584–10589.
305 W. Y. Chen, J. Y. Lin, W. J. Chen, L. Y. Luo, E. W. G. Diau and Y. C. Chen, *Nanomedicine*, 2010, **5**, 755–764.
306 Y. H. Lin and W. L. Tseng, *Anal. Chem.*, 2010, **82**, 9194–9200.
307 H. Kong, Y. X. Lu, H. Wang, F. Wen, S. C. Zhang and X. R. Zhang, *Anal. Chem.*, 2012, **84**, 4258–4261.
308 Y. Tao, Y. H. Lin, Z. Z. Huang, J. S. Ren and X. G. Qu, *Adv. Mater.*, 2013, **25**, 2594–2599.
309 A. Baksi, P. L. Xavier, K. Chaudhari, N. Goswami, S. K. Pal and T. Pradeep, *Nanoscale*, 2013, **5**, 2009–2016.
310 Y. Xu, J. Sherwood, Y. Qin, D. Crowley, M. Bonizzoni and Y. Bao, *Nanoscale*, 2014, **6**, 1515–1524.
311 A. Baksi, T. Pradeep, B. Yoon, C. Yannouleas and U. Landman, *ChemPhysChem*, 2013, **14**, 1272–1282.
312 D. Lu, L. Liu, F. Li, S. Shuang, Y. Li, M. M. F. Choic and C. Dong, *Spectrochim. Acta, Part A*, 2014, **121**, 77–80.
313 C.-J. Yu, T.-H. Chen, J.-Y. Jiang and W.-L. Tseng, *Nanoscale*, 2014, **6**, 9618–9624.

314 P. H. Chan, S. Y. Wong, S. H. Lin and Y. C. Chen, *Rapid Commun. Mass Spectrom.*, 2013, **27**, 2143–2148.
315 T. H. Chen, C. Y. Lu and W. L. Tseng, *Talanta*, 2013, **117**, 258–262.
316 A. Baksi and T. Pradeep, *Nanoscale*, 2013, **5**, 12245–12254.
317 S. S. Narayanan and S. K. Pal, *J. Phys. Chem. C*, 2008, **112**, 4874–4879.
318 T. Ueno, T. Koshiyama, T. Tsuruga, T. Goto, S. Kanamaru, F. Arisaka and Y. Watanabe, *Angew. Chem., Int. Ed.*, 2006, **45**, 4508–4512.
319 M. Knez, A. M. Bittner, F. Boes, C. Wege, H. Jeske, E. Maiβ and K. Kern, *Nano Lett.*, 2003, **3**, 1079–1082.
320 L. Rastogi and J. Arunachalam, *Colloids Surf., B*, 2013, **108**, 134–141.
321 S. Gautam, P. Dubey and M. N. Gupta, *Colloids Surf., B*, 2013, **102**, 879–883.
322 M. S. Bakshi, H. Kaur, T. S. Banipal, N. Singh and G. Kaur, *Langmuir*, 2010, **26**, 13535–13544.
323 G. Wei, F. Xu, Z. Li and K. D. Jandt, *J. Phys. Chem. C*, 2011, **115**, 11453–11460.
324 T. Yang, Y. Zhang and Z. Li, *Biomacromolecules*, 2011, **12**, 2027–2031.
325 Y. Lee and K. E. Geckeler, *J. Biomed. Mater. Res., Part A*, 2012, **100**, 848–855.
326 R. Das, R. Jagannathan, C. Sharan, U. Kumar and P. Poddar, *J. Phys. Chem. C*, 2009, **113**, 21493–21500.
327 H. Cai and P. Yao, *Nanoscale*, 2013, **5**, 2892–2900.
328 D. M. Eby, N. M. Schaeublin, K. E. Farrington, S. M. Hussain and G. R. Johnson, *ACS Nano*, 2009, **3**, 984–994.
329 M. Fujiwara, K. Shiokawa, M. Araki, N. Ashitaka, K. Morigaki, T. Kubota and Y. Nakahara, *Cryst. Growth Des.*, 2010, **10**, 4030–4037.
330 X. Q. Wang, H. L. Sun, Y. Q. Xia, C. X. Chen, H. Xu, H. H. Shan and J. R. Lu, *J. Colloid Interface Sci.*, 2009, **332**, 96–103.
331 A. E. Voinescu, D. Touraud, A. Lecker, A. Pfitzner, W. Kunz and B. W. Ninham, *Langmuir*, 2007, **23**, 12269–12274.
332 K. Zhao, M. Wang, X. Q. Wang, C. M. Wu, H. Xu and J. R. Lu, *Cryst. Growth Des.*, 2013, **13**, 1583–1589.
333 C. Jimenez-Lopez, A. Rodriguez-Navarro, J. M. Dominguez-Vera and J. M. Garcia-Ruiz, *Geochim. Cosmochim. Acta*, 2003, **67**, 1667–1676.
334 M. B. Cardoso, H. R. Luckarift, V. S. Urban, H. O'Neill and G. R. Johnson, *Adv. Funct. Mater.*, 2010, **20**, 3031–3038.
335 Y. Jiang, D. Yang, L. Zhang, Y. Jiang, Y. Zhang, J. Li and Z. Jiang, *Ind. Eng. Chem. Res.*, 2008, **47**, 1876–1882.
336 L. Zhang, D. Z. Qin, Q. R. Liu and G. X. He, *Micro Nano Lett.*, 2012, **7**, 115–117.
337 D. Z. Qin, L. Zhang, G. X. He and Q. R. Liu, *Mater. Lett.*, 2012, **66**, 7–9.
338 L. Zhang, G. R. Yang, G. X. He, L. Wang, Q. R. Liu, Q. X. Zhang and D. Z. Qin, *Appl. Surf. Sci.*, 2012, **258**, 8185–8191.
339 L. N. Hassani, F. Hindre, T. Beuvier, B. Calvignac, N. Lautram, A. Gibaud and F. Boury, *J. Mater. Chem. B*, 2013, **1**, 4011–4019.
340 X. He, L. Gao and N. Ma, *Sci. Rep.*, 2013, **3**, 2825.
341 H. Wei and E. Wang, *Chem. Lett.*, 2007, **36**, 210–211.
342 H. Wei, J. Liu, L. Zhou, J. Li, X. Jiang, J. Kang, X. Yang, S. Dong and E. Wang, *Chem.–Eur. J.*, 2008, **14**, 3687–3693.
343 H. Wei, L. L. Zhou, J. Li, J. F. Liu and E. K. Wang, *J. Colloid Interface Sci.*, 2008, **321**, 310–314.
344 D. Ivnitski, K. Artyushkova, R. A. Rincón, P. Atanassov, H. R. Luckarift and G. R. Johnson, *Small*, 2008, **4**, 357–364.
345 T. M. Garakani, H. Wang, T. Krappitz, B. M. Liebeck, P. van Rijn and A. Boker, *Chem. Commun.*, 2012, **48**, 10210–10212.
346 T. Shiomi, T. Tsunoda, A. Kawai, F. Mizukami and K. Sakaguchi, *Chem. Commun.*, 2007, 4404–4406.
347 T. Shiomi, T. Tsunoda, A. Kawai, H. Chiku, F. Mizukami and K. Sakaguchi, *Chem. Commun.*, 2005, 5325–5327.
348 F. Gao, Q. Lu and S. Komarneni, *Chem. Commun.*, 2005, 531–533.
349 Y. Takeda, T. Kondow and F. Mafune, *Chem. Phys. Lett.*, 2011, **504**, 175–179.
350 T. Koshiyama, N. Kawaba, T. Hikage, M. Shirai, Y. Miura, C. Y. Huang, K. Tanaka, Y. Watanabe and T. Ueno, *Bioconjugate Chem.*, 2010, **21**, 264–269.
351 M. Liang, L. B. Wang, R. X. Su, W. Qi, M. F. Wang, Y. J. Yu and Z. M. He, *Catal. Sci. Technol.*, 2013, **3**, 1910–1914.
352 M. Liang, L. B. Wang, X. Liu, W. Qi, R. X. Su, R. L. Huang, Y. J. Yu and Z. M. He, *Nanotechnology*, 2013, **24**, 245601.
353 P. G. Vekilov, *Nat. Nanotechnol.*, 2011, **6**, 82–83.
354 O. L. Muskens, M. W. England, L. Danos, M. Li and S. Mann, *Adv. Funct. Mater.*, 2013, **23**, 281–290.
355 Y. Takeda and F. Mafune, *Chem. Phys. Lett.*, 2014, **604**, 110–115.
356 H. Tabe, S. Abe, T. Hikage, S. Kitagawa and T. Ueno, *Chem.–Asian J.*, 2014, **9**, 1373–1378.
357 T. Koshiyama, M. Shirai, T. Hikage, H. Tabe, K. Tanaka, S. Kitagawa and T. Ueno, *Angew. Chem., Int. Ed.*, 2011, **50**, 4849–4852.
358 N. Yokoi, H. Inaba, M. Terauchi, A. Z. Stieg, N. J. M. Sanghamitra, T. Koshiyama, K. Yutani, S. Kanamaru, F. Arisaka, T. Hikage, A. Suzuki, T. Yamane, J. K. Gimzewski, Y. Watanabe, S. Kitagawa and T. Ueno, *Small*, 2010, **6**, 1873–1879.
359 T. Ueno, H. Tabe and Y. Tanaka, *Chem.–Asian J.*, 2013, **8**, 1646–1660.
360 T. Ueno, M. Abe, K. Hirata, S. Abe, M. Suzuki, N. Shimizu, M. Yamamoto, M. Takata and Y. Watanabe, *J. Am. Chem. Soc.*, 2009, **131**, 5094–5100.
361 B. Wang, C. L. Guo, G. J. Chen, B. Park and B. Q. Xu, *Chem. Commun.*, 2012, **48**, 1644–1646.
362 C. L. Guo, B. Wang, L. C. Wang and B. Q. Xu, *Chem. Commun.*, 2012, **48**, 12222–12224.
363 M. J. Han, H. Yun and S. Y. Lee, *Biotechnol. Adv.*, 2008, **26**, 591–609.

364 A. Y. Chen, Z. T. Deng, A. N. Billings, U. O. S. Seker, M. Y. Lu, R. J. Citorik, B. Zakeri and T. K. Lu, *Nat. Mater.*, 2014, **13**, 515–523.
365 M. V. Cespedes, U. Unzueta, W. Tatkiewicz, A. Sanchez-Chardi, O. Conchillo-Sole, P. Alamo, Z. K. Xu, I. Casanova, J. L. Corchero, M. Pesarrodona, J. Cedano, X. Daura, I. Ratera, J. Veciana, N. Ferrer-Miralles, E. Vazquez, A. Villaverde and R. Mangues, *ACS Nano*, 2014, **8**, 4166–4176.
366 J. Grzyb, *Acta Phys. Pol., A*, 2012, **122**, 279–283.